

PROJECT 3

FYS3150 - COMPUTATIONAL PHYSICS

Quantum dots

Author:
Vidar SKOGVOLL

Candidate:
32

December 7, 2014

Abstract

Variational Monte Carlo has been implemented to find upper bounds on the energy of electrons in a harmonic oscillator trap. The Metropolis algorithm was implemented, both in a brute force way and using importance sampling. Numerical and analytical expressions was used for the energy functions and the quantum force. These different ways of solving the problem are referred to as "methods".

The brute force method with numerical expressions was verified for 2,6 and 12 electrons without electron repulsion against known benchmarks. Then the energy for the 2 electron case with repulsion was found to be $3.00022 J_0$ (Unit: see section 2.1.1), a value very close to the analytical solution of $3 J_0$ credited to Taut [4]. As a third verification, the different methods produced the same results when given the same problem parameters.

Then some optimizations and computational aspects was looked at. The importance of the Jastrow factor was investigated and shown to decrease with oscillator strength. Importance sampling yielded a large acceptance ratio and seemed stable around a time step of $\delta t = 10^{-2} s_0$. As for time usage, the brute force method with analytical expressions was the fastest and proved almost 20 times faster than the least efficient method.

Finally, some properties of the optimal wave functions was investigated and the virial theorem was tested for both with and without repulsion. The theorem held for the non-repulsion oscillator but not for the oscillator with electron repulsion.

Contents

1	Introduction	4
2	Theory	4
2.1	The physical system	4
2.1.1	Natural units	4
2.1.2	The quantum mechanics and the variational principle	5
2.1.2.1	The quantum mechanics	5
2.1.2.2	The variational principle	6
2.1.2.3	Finding the expectation value of \hat{H}	6
2.1.2.4	Verifying that we have found an eigenstate	7
2.1.3	The test function Ψ_T	8
2.1.3.1	The modified Slater determinant $\text{Det}_M(\phi_0, \dots, \phi_{N-1})$	8
2.1.3.2	The Jastrow factor $J(\vec{r}_0, \dots, \vec{r}_{N-1})$	9
2.1.3.3	Motivation	9
2.1.3.4	Closed form expression of the local energy	10
2.1.4	The virial theorem	11
2.2	The numerical foundation	12
2.2.1	Monte Carlo simulations	12
2.2.2	The Metropolis algorithm	12
2.2.2.1	Brute force Metropolis	14

2.2.2.2	Importance sampling	14
2.2.2.3	Application of the variational Monte Carlo method	15
2.2.3	Parallelization	17
3	Experimental	19
3.1	Benchmarks and verification	19
3.1.1	Benchmarks for the brute force approach, no repulsion or Jastrow factor .	19
3.1.2	Benchmark for the brute force approach, with repulsion and Jastrow factor	19
3.1.3	Comparison of different methods	19
3.2	Optimization and differences	20
3.2.1	Test cases	20
3.2.2	Jastrow factor	20
3.2.3	Importance sampling	20
3.2.4	Timely differences between methods	21
3.3	Applications	21
3.3.1	Properties of the approximated wave functions	21
3.3.2	The virial theorem	21
4	Results and discussion	22
4.1	Benchmarks and verification	22
4.1.1	Benchmarks for the brute force approach, no repulsion or Jastrow factor .	22
4.1.2	Benchmark for the brute force approach, with repulsion and Jastrow factor	23
4.1.3	Comparison of different methods	23
4.2	Optimization and differences	25
4.2.1	Test cases	25
4.2.2	Jastrow factor	25
4.2.3	Importance sampling	27
4.2.4	Timely differences between methods	28
4.2.5	Discussion: code efficiency and time constraints	31
4.3	Applications	32
4.3.1	Properties of the approximated wave functions	32
4.3.2	The virial theorem	33
5	Conclusion	35
Appendix A Reference to the questions posed in the project instructions		37
Appendix B Code		38

1 Introduction

Quantum theory is often thought of as "the most precisely tested and most successful theory in the history of science"¹, which is not a controversial statement. Whereas the mathematical foundation upon which it is built is more or less the same today as it was 50 years ago, the computational power available to us has grown exponentially the last 30 years, allowing us to explore the mysteries of quantum systems within a couple of minutes of computational time. The work presented in this paper demonstrates how computational power is an excellent tool to solve difficult quantum mechanical problems.

In this project I have used the variational Monte Carlo method to find upper bounds on energies on a system of 2, 6 and 12 electrons in a 2-dimensional harmonic oscillator trap, often called *quantum dots*. Three classes have been constructed in the c++-language which construct the problem and investigates the interesting properties using several CPU's in parallel. The different methods presented in this report all managed to correctly solve the quantum mechanical problem, but the fastest method was almost 20 times faster than the slowest method, illustrating that much computation time can be saved by smart programming. This is very important since many challenges in physics today are very complex problems such as the 24-dimensional integral solved in this report (for the 12-electron case). If we were to evaluate this integral with 10 grid points for each dimension, this would mean a total of 10^{24} grid points, for which a standard computer CPU might require the age of the universe in order to finish calculation.

The simulations showed some expected results, for example the reproduction certain energy benchmarks, but also some other interesting features. It turns out that the electron correlations (i.e. the importance of the electron repulsion) decreases with the strength of the harmonic oscillator. This is a strange result because normally, one would think that the electron repulsion becomes *more* important as the electrons are "squeezed" together, but in fact it is the opposite that is true. Also, the virial theorem was verified for the non-repulsive harmonic oscillator, but shown to not hold when including the electron-repulsion part. It seems as if the electrons "freeze" in place when the oscillator potential gets too weak.

2 Theory

This section will provide the theory needed to understand the content of this report.

2.1 The physical system

This section will explain the physics of the project.

2.1.1 Natural units

Throughout the project, *natural units*² are used with $\hbar = c = e = m_e = 1$. Setting these constants equal to one automatically sets the length, energy and time scale of the system. Three of these constants are given in SI-units by

¹http://www.4physics.com/phy_demo/QM_Article/article.html

²http://en.wikipedia.org/wiki/Natural_units

$$c = 3.00 \times 10^8 \frac{\text{m}}{\text{s}} \quad (2.1.1)$$

$$\hbar = 1.05 \times 10^{-34} \frac{\text{kg} \cdot \text{m}^2}{\text{s}} \quad (2.1.2)$$

$$m_e = 9.11 \times 10^{-31} \text{ kg} \quad (2.1.3)$$

Since these constants are set to 1 we can deduce that the unit m_0 of length is given by

$$\text{m}_0 = \frac{\hbar}{m_e c} = \frac{1.05 \times 10^{-34} \frac{\text{kg} \cdot \text{m}^2}{\text{s}}}{9.11 \times 10^{-31} \text{ kg} \cdot 3.00 \times 10^8 \frac{\text{m}}{\text{s}}} = 3.84 \times 10^{-13} \text{ m} \quad (2.1.4)$$

The unit of time s_0 can be equivalently shown to be

$$\text{s}_0 = \frac{\text{m}_0}{c} = \frac{3.84 \times 10^{-13} \text{ m}}{3.00 \times 10^8 \frac{\text{m}}{\text{s}}} = 1.28 \times 10^{-21} \text{ s} \quad (2.1.5)$$

The unit of energy J_0 becomes

$$\text{J}_0 = \frac{\hbar}{\text{s}_0} = \frac{1.05 \times 10^{-34} \text{ J} \cdot \text{s}}{1.28 \times 10^{-21} \text{ s}} = 8.20 \times 10^{-14} \text{ J} \quad (2.1.6)$$

And finally, the unit of the oscillator frequency Hz_0 is thus

$$\text{Hz}_0 = \frac{1}{\text{s}_0} = 7.81 \times 10^{20} \text{ Hz} \quad (2.1.7)$$

2.1.2 The quantum mechanics and the variational principle

2.1.2.1 The quantum mechanics

In this project we will look at a system of N electrons in a so-called *quantum dot*. That is, a two dimensional harmonic oscillator with potential

$$V(\vec{r}) = \frac{1}{2} \omega^2 r^2 \quad (2.1.8)$$

This potential gives rise to a multi-particle Hamiltonian \hat{H} given as the sum of an ordinary Hamiltonian and an electron repulsive part

$$\hat{H} = \sum_{i=1}^N \left(-\frac{1}{2} \nabla_i^2 + \frac{1}{2} \omega^2 r_i^2 \right) + \sum_{i < j} \frac{1}{r_{ij}} \quad (2.1.9)$$

Where $r_{ij} = |\vec{r}_i - \vec{r}_j|$ is the distance between the electrons i and j and $r_i = |\vec{r}_i| = \sqrt{x_i^2 + y_i^2}$ when $\vec{r}_i = \begin{pmatrix} x_i \\ y_i \end{pmatrix}$. Our goal in this project is to find the ground eigenstate and energy of this multi-particle Hamiltonian numerically.

2.1.2.2 The variational principle

We will approach this by constructing a real test function $\Psi_T(\vec{r}_0, \vec{r}_1, \dots, \vec{r}_{N-1}, \alpha, \beta)$ dependent on two parameters α and β and calculate the expectation value of the Hamiltonian operator $\langle \hat{H} \rangle$. As we know, the orthonormal eigenstates Ψ_i of the Hamiltonian forms a complete basis, so any state, including our test state Ψ_T , can be written as a linear combination of the eigenstates

$$\Psi_T = \sum_i c_i \Psi_i \quad (2.1.10)$$

Inserting this expression into the equation for the expectation value of \hat{H} gives

$$\begin{aligned} \langle \hat{H} \rangle &= \frac{\int \Psi_T \hat{H} \Psi_T d\vec{r}}{\int \Psi_T \Psi_T d\vec{r}} = \frac{\int (\sum_i c_i^* \Psi_i^*) \hat{H} (\sum_i c_i \Psi_i) d\vec{r}}{\int (\sum_i c_i^* \Psi_i^*) (\sum_i c_i \Psi_i) d\vec{r}} = \frac{\int (\sum_i c_i^* \Psi_i^*) (\sum_i c_i E_i \Psi_i) d\vec{r}}{\int (\sum_i c_i^* \Psi_i^*) (\sum_i c_i \Psi_i) d\vec{r}} \\ &= \frac{\sum_i |c_i|^2 E_i}{\sum_i |c_i|^2} \end{aligned} \quad (2.1.11)$$

The energy of the ground state E_0 is smaller than all other E_i 's so

$$\frac{\sum_i |c_i|^2 E_i}{\sum_i |c_i|^2} \geq \frac{\sum_i |c_i|^2 E_0}{\sum_i |c_i|^2} = E_0 \frac{\sum_i |c_i|^2}{\sum_i |c_i|^2} = E_0 \quad (2.1.12)$$

$$\boxed{\langle H \rangle \geq E_0} \quad (2.1.13)$$

This simple observation is called *the variational principle* and is what we will use to narrow our search for the optimal parameters α and β . We will look for the parameters α and β that gives us the smallest value of $\langle \hat{H} \rangle$ and this will be our estimate for the ground state energy. The corresponding trial wave function will be our approximation for the ground state wave function of the system.

2.1.2.3 Finding the expectation value of \hat{H}

We have

$$\langle \hat{H} \rangle = \frac{\int \Psi_T \hat{H} \Psi_T d\vec{r}}{\int \Psi_T \Psi_T d\vec{r}} = \int \frac{\Psi_T \Psi_T}{\int \Psi_T \Psi_T d\vec{r}} \frac{1}{\Psi_T} \hat{H} \Psi_T d\vec{r} \quad (2.1.14)$$

If we rename probability density function of the particles

$$\boxed{\frac{\Psi_T \Psi_T}{\int \Psi_T \Psi_T d\vec{r}} = P(\vec{r})} \quad (2.1.15)$$

And introduce the local energy

$$\boxed{E_L(\vec{r}) = \frac{1}{\Psi_T} \hat{H} \Psi_T} \quad (2.1.16)$$

The integral becomes

$$\boxed{\langle \hat{H} \rangle = \int P(\vec{r}) E_L(\vec{r}) d\vec{r} = \langle E_L \rangle} \quad (2.1.17)$$

Thus, to calculate the expectation value of \hat{H} we can just calculate the expectation value of the local energy.

2.1.2.4 Verifying that we have found an eigenstate

We could very well find a minimum of $\langle \hat{H} \rangle$ that is not an eigen energy of the system, i.e. still larger than E_0 . To address this problem, let's look at the variance V_{E_L} of $\langle E_L \rangle$.

$$V_{E_L} = \langle E_L^2 \rangle - \langle E_L \rangle^2 = \int P(\vec{r}) \left(\frac{1}{\Psi_T} \hat{H} \Psi_T \right)^2 d\vec{r} - \left(\int P(\vec{r}) \frac{1}{\Psi_T} \hat{H} \Psi_T d\vec{r} \right)^2 \quad (2.1.18)$$

Since

$$\begin{aligned} \langle (E_L - \langle E_L \rangle)^2 \rangle &= \langle E_L^2 - 2E_L \langle E_L \rangle + \langle E_L \rangle^2 \rangle = \langle E_L^2 \rangle - 2\langle E_L \rangle \langle E_L \rangle + \langle E_L \rangle^2 \\ &= \langle E_L^2 \rangle - \langle E_L \rangle^2 = V_{E_L} \end{aligned} \quad (2.1.19)$$

We have that if $V_{E_L} = 0$, then

$$\langle (E_L - \langle E_L \rangle)^2 \rangle = 0 \quad (2.1.20)$$

$$0 = \int \left(P(\vec{r}) E_L(\vec{r}) - \int P(\vec{r}) E_L(\vec{r}) d\vec{r} \right)^2 d\vec{r} = \int \left(\frac{1}{\Psi_T} \hat{H} \Psi_T - \int \Psi_T \hat{H} \Psi_T d\vec{r} \right)^2 d\vec{r} \quad (2.1.21)$$

When the Hamiltonian acts on a real function, it gives a real function. And since Ψ_T is real $\frac{1}{\Psi_T} \hat{H} \Psi_T - \int \Psi_T \hat{H} \Psi_T d\vec{r}$ is real. By consequence

$$\left(\frac{1}{\Psi_T} \hat{H} \Psi_T - \int \Psi_T \hat{H} \Psi_T d\vec{r} \right)^2 > 0 \quad (2.1.22)$$

Which means that for the integral in equation 2.1.21 to be zero, the following must be true for all \vec{r}

$$\frac{1}{\Psi_T} \hat{H} \Psi_T - \int \Psi_T \hat{H} \Psi_T d\vec{r} = 0 \quad (2.1.23)$$

$$\Psi_T \hat{H} \Psi_T = \int \Psi_T \hat{H} \Psi_T d\vec{r} \quad (2.1.24)$$

The right hand side of this equation is just a real number. Naming this number E gives

$$\frac{1}{\Psi_T} \hat{H} \Psi_T = E \quad (2.1.25)$$

$$\boxed{\hat{H} \Psi_T = E \Psi_T} \quad (2.1.26)$$

Which is nothing but the eigenvalue equation stating that Ψ_T is an eigenstate of \hat{H} . This will serve as a test to see if the state we have found when minimizing the expectation value of E_L is an eigenstate of the Hamilton operator. It is just as easily (perhaps easier) shown that if Ψ_T is an eigenstate of \hat{H} , then the variance of the local energy is 0. This means that if the variance of our test function is *not* 0, then it is *not* an eigenfunction of \hat{H} . We can summarize this discussion as follows

$$\boxed{V_{E_L} = 0 \quad \text{if and only if} \quad \Psi_T \text{ is an eigenstate of } \hat{H}} \quad (2.1.27)$$

2.1.3 The test function Ψ_T

We will in this project use the trial wave functions of $\vec{r}_i = \begin{pmatrix} x_i \\ y_i \end{pmatrix}$ given by

$$\boxed{\Psi_T(\vec{r}_0, \dots, \vec{r}_{N-1}) = \text{Det}_M(\phi_0, \dots, \phi_{N-1}) \cdot J(\vec{r}_0, \dots, \vec{r}_{N-1})} \quad (2.1.28)$$

2.1.3.1 The modified Slater determinant $\text{Det}_M(\phi_0, \dots, \phi_{N-1})$

$\text{Det}_M(\phi_0, \dots, \phi_{N-1})$ is a modified *Slater determinant* defined as

$$\boxed{\begin{aligned} &\text{Det}_M(\phi_0, \dots, \phi_{N-1}) = |U| \cdot |D| \\ = &\begin{vmatrix} \phi_0(\vec{r}_0) & \phi_2(\vec{r}_0) & \dots & \phi_{N-2}(\vec{r}_0) \\ \phi_0(\vec{r}_2) & \phi_2(\vec{r}_2) & \dots & \phi_{N-2}(\vec{r}_2) \\ \dots & \dots & \dots & \dots \\ \phi_0(\vec{r}_{N-2}) & \phi_2(\vec{r}_{N-2}) & \dots & \phi_{N-2}(\vec{r}_{N-2}) \end{vmatrix} \cdot \begin{vmatrix} \phi_1(\vec{r}_1) & \phi_3(\vec{r}_1) & \dots & \phi_{N-1}(\vec{r}_1) \\ \phi_1(\vec{r}_3) & \phi_3(\vec{r}_3) & \dots & \phi_{N-1}(\vec{r}_3) \\ \dots & \dots & \dots & \dots \\ \phi_1(\vec{r}_{N-1}) & \phi_3(\vec{r}_{N-1}) & \dots & \phi_{N-1}(\vec{r}_{N-1}) \end{vmatrix} \end{aligned}} \quad (2.1.29)$$

Where $\phi_i(\vec{r}_i)$ is a wave function resembling one of the eigenfunctions of the Hamilton operator for *one* particle in a two dimensional harmonic oscillator, but parameterized by α in the following way:

$$\boxed{\phi_i(\vec{r}_j) = H_{n_x}(\sqrt{\alpha\omega}x_j)H_{n_y}(\sqrt{\alpha\omega}y_j)\exp(-\alpha\omega(x^2 + y^2)/2)} \quad (2.1.30)$$

Where $H_n(x)$ is the n th Hermite polynomial³ of x . The reason for this modified version of the Slater determinant (whose real form can be explored elsewhere⁴) is that the spin parts of the wave functions are not incorporated in the expressions of $\phi_i(\vec{r}_j)$. The result is that if we were to insert these into a regular Slater determinant we would get 0, every time. The modified Slater determinant Det_M avoids this issue while still conserving some of the most important properties of the Slater determinant.

$n_x(i)$ and $n_y(i)$ corresponds to the quantum numbers needed to "fill up" the system from the lowest energy levels twice (one for each spin configuration). For $i < 12$, the explicit dependence of n_x, n_y on i is given in table 2.1.1.

³http://en.wikipedia.org/wiki/Hermite_polynomials

⁴http://en.wikipedia.org/wiki/Slater_determinant

$i =$	0	1	2	3	4	5	6	7	8	9	10	11
$n_x =$	0	0	1	1	0	0	2	2	1	1	0	0
$n_y =$	0	0	0	0	1	1	0	0	1	1	2	2

Table 2.1.1: The explicit dependence of n_x and n_y on i in the construction of the trial wave functions.

2.1.3.2 The Jastrow factor $J(\vec{r}_0, \dots, \vec{r}_{N-1})$

$J(\vec{r}_0, \dots, \vec{r}_{N-1})$ is a so-called *Jastrow factor*, which represents the electron repulsion part of the wave function, defined as

$$J(\vec{r}_0, \dots, \vec{r}_{N-1}) = \prod_{i < j}^N \exp\left(\frac{a_{ij} r_{ij}}{1 + \beta r_{ij}}\right) \quad (2.1.31)$$

where $r_{ij} = |\vec{r}_i - \vec{r}_j|$ and $a_{ij} = \begin{cases} 1/3 & \text{if spin(i) and spin(j) are parallel} \\ 1 & \text{if spin(i) and spin(j) are anti-parallel} \end{cases}$

When calculating the local energy for the perturbed potential, there arises a singularity when $r_{ij} \rightarrow 0$. This is not physical, and the way the Jastrow factor is designed it cancels this singularity when taken the derivative of. Therefore, we might expect the Jastrow factor to play a bigger role in the physical systems where the interaction (or often called correlation) between the electrons is bigger. We will use the relative difference between the energy obtained with the Jastrow factor to that obtained without as a measure of the interaction between the electrons.

2.1.3.3 Motivation

The motivation of such a trial wave function is that it resembles the unperturbed harmonic oscillator eigenstates. See figure 2.1.1.

The energies of these levels are given by the well known 2D-harmonic oscillator energy formula

$$E_{n_x, n_y} = \hbar\omega(1 + n_x + n_y) \quad (2.1.32)$$

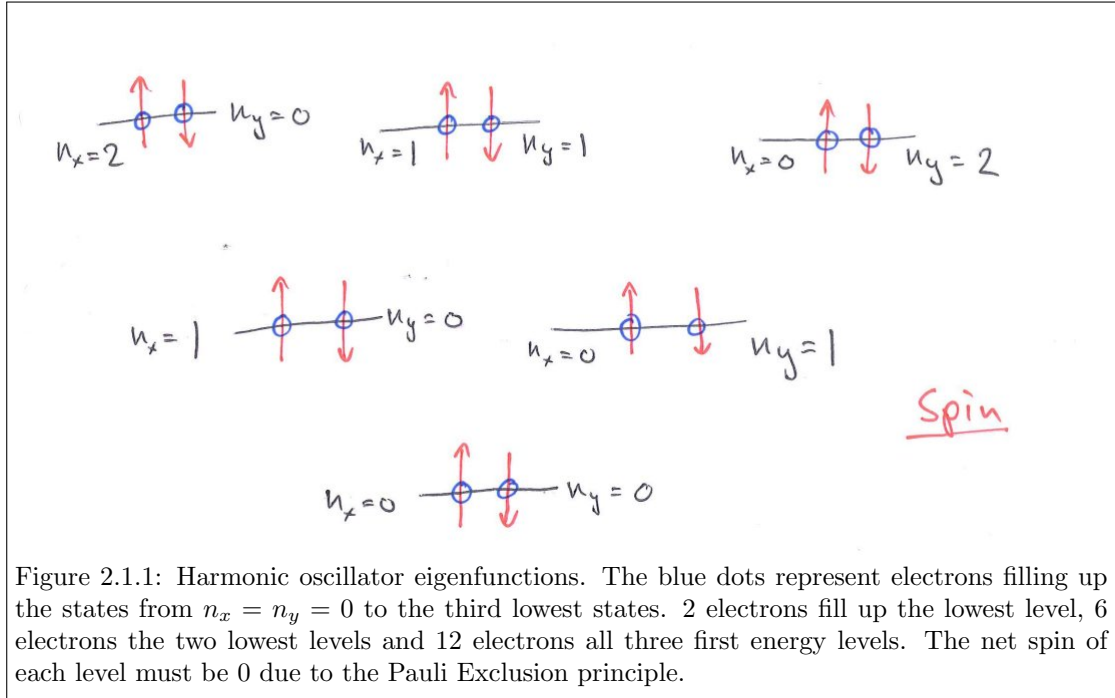
So if we have two electrons in the lowest state ($n_x = n_y = 0$), we would expect the energy of this state to be

$$2 \cdot \hbar\omega(1 + 0 + 0) = 2\hbar\omega = 2\omega \quad (2.1.33)$$

When using natural units.

To have two electrons in the same state, their spin must be opposite due to the Pauli exclusion principle. This means that the total spin of the $n_x = n_y = 0$ state is 0. It can be shown that the wave function given by equation 2.1.28 when $N = 2$ (i.e. two electrons) is given by the following equation

$$\Psi_T(\vec{r}_0, \vec{r}_1) = \exp(-\alpha\omega(r_0^2 + r_1^2)/2) \cdot J \quad (2.1.34)$$



If we do not include the repulsion part of the system, there is no need to include the Jastrow factor. It can be shown that this state is an eigenstate of the unperturbed harmonic oscillator with energy 2ω when $\alpha = 1$. This analogy can be extended to the $N = 6$ and $N = 12$ electron case as well. When $N = 6$ the unperturbed energy should be the sum of the energies in the first level (i.e. 2ω) and the collective energies of the electrons in the second level states ($n_x = 1, n_y = 0 \vee n_x = 0, n_y = 1$) which is $4 \cdot 2\omega = 8\omega$, resulting in a total energy of 10ω . Equivalently, the energy for the $N = 12$ electron case should be 28ω . These energies will all serve as benchmarks and we should get the exact results when there is no repulsion, $\alpha = 1$ and the Jastrow factor is omitted.

2.1.3.4 Closed form expression of the local energy

To evaluate the local energy

$$E_L(\vec{r}) = \frac{1}{\Psi_T} \hat{H} \Psi_T = \frac{1}{\Psi_T} \left(\sum_i -\frac{1}{2} \nabla_i^2 + \sum_i V(\vec{r}_i) \right) \Psi_T = \sum_i V(\vec{r}_i) - \frac{1}{2} \sum_i \frac{1}{\Psi_T} \nabla_i^2 \Psi_T \quad (2.1.35)$$

We need a lot of computational power. This is mainly due to the fact that we need to compute the sum of the laplacian operators on each particle. This is an easy task to do "brute force", but if we were able to find an analytical expression for the local energy, it could possibly simplify calculations by a lot. Let's look at one of the terms in the laplacian sum, naming it *LSP* (Laplacian sum part)

$$LSP = \frac{1}{\Psi_T} \nabla_i^2 \Psi_T \quad (2.1.36)$$

Inserting the trial wave function expression (equation 2.1.28) into the latter gives

$$\frac{1}{\Psi_T} \nabla_i^2 \Psi_T = \frac{1}{\text{Det}_M J} \nabla_i^2 (\text{Det}_M J) \quad (2.1.37)$$

The function Det_M is a product of two matrix-determinants $|U|$ and $|D|$ where $|U|$ handles all the particles assigned spin up and $|D|$ the ones assigned spin down. Particle i has either spin up or down, so let $|S_i|$ denote the matrix determinant which handles particle i and $|S_{j \neq i}|$ denote the one that doesn't, then

$$\frac{1}{\Psi_T} \nabla_i^2 \Psi_T = \frac{1}{|S_i| |S_{j \neq i}| J} \nabla_i^2 (|S_i| |S_{j \neq i}| J) = \frac{1}{|S_i| |S_{j \neq i}| J} |S_{j \neq i}| \nabla_i^2 (|S_i| J) = \frac{1}{|S_i| J} \nabla_i^2 (|S_i| J) \quad (2.1.38)$$

Using the product rule of the laplacian operator gives

$$\boxed{\frac{1}{\Psi_T} \nabla_i^2 \Psi_T = \frac{\nabla_i^2 |S_i|}{|S_i|} + \frac{\nabla_i^2 J}{J} + 2 \frac{\nabla_i J}{J} \cdot \frac{\nabla_i |S_i|}{|S_i|}} \quad (2.1.39)$$

It is possible to find analytical expression for all these terms, and that has been already been done in a master thesis written by Jørgen Høgberget [3]. The arguments will not be repeated but the results are as follows (with names added for code reference)

$$NSS = \frac{\nabla_i |S_i|}{|S_i|} = \sum_{k=0}^{N/2} [(S^{-1})_{ki} \cdot \nabla_i \phi_{2k}(\vec{r}_i)] \quad (2.1.40a)$$

$$N2SS = \frac{\nabla_i^2 |S_i|}{|S_i|} = \sum_{k=0}^{N/2} [(S^{-1})_{ki} \cdot \nabla_i^2 \phi_{2k}(\vec{r}_i)] \quad (2.1.40b)$$

$$NJJ = \frac{\nabla_i J}{J} = \sum_{k \neq i} \frac{a_{ik}}{r_{ik}} \frac{\vec{r}_i - \vec{r}_k}{(1 + \beta r_{ik})^2} \quad (2.1.40c)$$

$$N2JJ = \frac{\nabla_i^2 J}{J} = \left| \frac{\nabla_i J}{J} \right|^2 + \sum_{k \neq i} \frac{a_{ik}}{r_{ik}} \frac{1 - \beta r_{ik}}{(1 + \beta r_{ik})^3} \quad (2.1.40d)$$

$\nabla_i \phi_k(\vec{r}_i)$ and $\nabla_i^2 \phi_k(\vec{r}_i)$ scan be found simply by inserting and taking the derivative of the Hermite polynomials. The explicit formulas for ϕ_k for k in the range 0 to 11 is given in table 2.1.2 and are also taken from the master thesis by Jørgen Høgberget.

2.1.4 The virial theorem

The virial theorem proposes a proportionality between the expectation value of the total kinetic energy $\langle T \rangle$ and the expectation value of the total potential energy $\langle V \rangle$. For a pure (unperturbed) harmonic oscillator this proportionality is given by

k	(n_x, n_y)	$\phi_k(\vec{r})$	$\nabla_i \phi_k(\vec{r}_i) = [\nabla_x, \nabla_y]$	$\nabla_i^2 \phi_k(\vec{r}_i)$
0	(0,0)	1	$-[l^2 x, l^2 y]$	$l^2(l^2 r^2 - 2)$
2	(1,0)	$2lx$	$-2l[(lx - 1)(lx + 1), l^2 xy]$	$2l^3 x(l^2 r^2 - 4)$
4	(0,1)	$2ly$	$-2l[l^2 xy, (ly - 1)(ly + 1)]$	$2l^3 y(l^2 r^2 - 4)$
6	(2,0)	$4l^2 x^2 - 2$	$-2[l^2 x(2l^2 x^2 - 5), l^2 y(2l^2 x^2 - 1)]$	$2l^2(l^2 r^2 - 6)(2l^2 x^2 - 1)$
8	(1,1)	$4l^2 xy$	$-4l^2[y(lx - 1)(lx + 1), x(ly - 1)(ly + 1)]$	$4l^4 xy(l^2 r^2 - 6)$
10	(0,2)	$4l^2 y^2 - 1$	$-2[l^2 x(2l^2 y^2 - 1), l^2 y(2l^2 y^2 - 5)]$	$2l^2(l^2 r^2 - 6)(2l^2 y^2 - 1)$

Table 2.1.2: Table of derivatives of $\phi_k(\vec{r}_i)$ where $l = \sqrt{\alpha\omega}$. The factor $e^{-\frac{1}{2}l^2 r^2}$ is omitted from all expressions. The formula for $k + 1$ is the same as for k if k is even (e.g. $\phi_0 = \phi_1$).

$$\langle T \rangle = \langle V \rangle \quad (2.1.41)$$

Thus, if the virial theorem holds for any harmonic potential strength ω , we would expect the ratio of $\langle T \rangle$ and $\langle V \rangle$ to remain constant as a function of ω . This has been investigated with and without repulsion in this report.

2.2 The numerical foundation

This section will provide the theory of the numerical foundation upon which this project is done.

2.2.1 Monte Carlo simulations

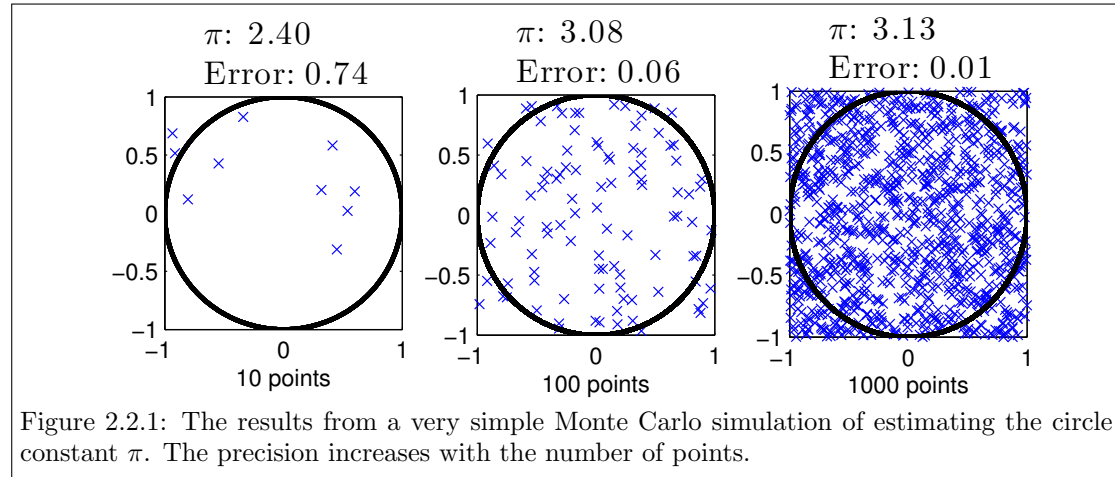
A Monte Carlo simulation is a way of solving a mathematical or physical problem by generating a random (or pseudo random⁵) sequence of numbers and evaluating some quantity on the assumption that the random sequence of numbers is representative of the domain of the physical system. An example is evaluating the area of the unit circle by randomly placing points in a $[-1, 1] \times [-1, 1]$ grid and find the fraction points whose distance to the origin is ≤ 1 and multiply this fraction by the area of the grid (i.e. 4). Such a simple Monte Carlo simulation can give the result as shown in figure 2.2.1.

However, the method is not confined to this sort of problem, but can be applied to a variety of mathematical and physical problems. In this report, the method, through the Metropolis algorithm (see section 2.2.2) has been applied to a quantum mechanical system.

2.2.2 The Metropolis algorithm

The Metropolis algorithm is a method which cleverly employs a stochastic approach in order to quickly estimate certain mathematical objects. The method is explained at lengths elsewhere[2], but in this section we will look at an example which captures the main idea of the method.

⁵Almost no electronic random number generator of today is truly random. The sequence of numbers generated will repeat itself after a long period. These periods however, are incredibly long and we will for this report consider the random number generators to be truly random.



Suppose we have a PDF⁶ $P(x)$ in a domain $[a, b]$ for which we want to calculate the expectation value $\langle g \rangle$ of some function $g(x)$. The integral we need to solve is then

$$\langle g \rangle = \int_a^b P(x)g(x)dx \quad (2.2.1)$$

This integral can be approximated as follows

$$\int_a^b P(x)g(x)dx \approx \frac{b-a}{N} \sum_i P(x_i)g(x_i) \equiv I \quad (2.2.2)$$

Where x_i are some uniformly chosen values in the interval $[a, b]$. Now, imagine instead of picking values x_i uniformly and weighing them by multiplying $g(x)$ with $P(x)$ instead chose the values of \tilde{x}_i from the PDF $P(x)$ and calculated the quantity \tilde{I} given by

$$\tilde{I} = \frac{1}{N} \sum_i g(\tilde{x}_i) \quad (2.2.3)$$

It can be shown mathematically that for large enough N , these two quantities I and \tilde{I} approach the same value. The problem with such an approach is that we need the precise expression for the PDF $P(x)$ and a robust algorithm for choosing random values from it. With the Metropolis algorithm however, we can use this approach *without* knowing the precise expression of the PDF and the relevant values from the domain come naturally.

The algorithm requires that we are able to calculate $\tilde{P}(x)$, an un-normalized version of $P(x)$ (i.e. some function $aP(x)$ proportional to $P(x)$). This may seem like a very strong requirement, but in many applications, as in this project, this is a much easier task than to calculate the precise PDF. The algorithm goes as follows. Starting with a position x choose a new trial position x_p by

$$x_p = x + \Delta x \quad (2.2.4)$$

⁶Probability Distribution Function

Where Δx is a random step according to some rule (see subsections). Then generate a probability criteria $s \in [0, 1]$. Now, if

$$\boxed{\frac{P(x_p)}{P(x)} = \frac{aP(x_p)}{aP(x)} = \frac{\tilde{P}(x_p)}{\tilde{P}(x)} \equiv w \geq s} \quad (2.2.5)$$

We accept the trial position as our new x and if not we reject it. If we choose new values of x_i in this manner, the collection of x_i 's will in fact reflect the PDF $P(x)$, which was what we needed in order to use equation 2.2.3. Note how equation 2.2.5 doesn't require us to have the exact form of the probability distribution function, only a function $\tilde{P}(x)$ proportional to it.

The intuition behind the algorithm is that for each new position x_i we generate is drawn towards the part of the domain where $P(x)$ is bigger. To see this, we note that if $P(x_p) > P(x)$ then $\frac{P(x_p)}{P(x)} > 1$ which is always bigger than $s \in [0, 1]$ and the new move is always accepted. Whereas if $P(x_p) < P(x)$, the move might be rejected. This allows new values of x_i to be chosen from where $P(x)$ is big, but at the same time allows values with lower values of $P(x)$ to be chosen. Which is what we expect from a PDF. The fact that for a large number M of such steps, the values x_i picked actually reflects the PDF requires some more mathematics, and once again we refer to the lecture notes of the course [2].

2.2.2.1 Brute force Metropolis

If we have no information about the physical nature of the system a reasonable way to model Δx is the following

$$\boxed{\Delta x = r\Delta x_0} \quad (2.2.6)$$

Where r is a random number between 0 and 1 and Δx_0 is a predefined step length. The step length Δx_0 is affecting the effectiveness of the algorithm in two contradicting ways. A small step length increases the probability of each suggested move x_p being accepted, but weakens the ergodicity⁷ of the method.

Since we have no physical understanding of the system when using the brute force Metropolis algorithm, we model our probability criteria s as a uniform random number between 0 and 1.

If the acceptance ratio is too low, then we are not moving away from the same point and the sampling becomes non-representative of the domain. However, if we have a too small step length resulting in a large acceptance rate, the steps taken are so small that we are also staying too long in one place, and thus not getting a proper representation of the domain. It can be argued that a good balance between these two aspects is to achieve an acceptance ratio (i.e. the ratio between accepted and rejected moves) of around 0.5.

This method is what will be called the "Brute Force Metropolis algorithm".

2.2.2.2 Importance sampling

If our current position x is in a region where the probability distribution is important, i.e. has a large value, a small step Δx would be favorable. This is because we want to sample many points

⁷The way in which the walker is able to reach all positions within a finite number of steps.

in this region, which is what a small step allows. In contrast, if the current position x is in an unimportant region, we want a large step Δx since we don't mind moving a bit farther from the region we're in. The brute force approach produced a step independent of the PDF value in each point, which resulted in an optimal acceptance ratio of around 0.5. If we could introduce some sort of rule which adjusts the step Δx according to the value of the PDF in the point we currently are, this could allow us to achieve a higher acceptance rate with the same ergodicity.

To make such a rule, we need to use our physical understanding of the system. One way of doing so is to consider the points to move as a random walker would where the resulting probability is equal to the PDF we're treating. Doing this, and invoking the Fokker-Planck and Langevin equations⁸, it can be shown that the choice of Δx is as follows

$$\Delta x = DF(x)\delta t + \eta \quad (2.2.7)$$

Where D is the diffusion term, $F(x)$ is a drift term which is responsible for pulling the particle towards regions where the PDF is important and η is a Gaussian random number with a variance of $2D\delta t$.

The metropolis algorithm relies, as we have seen, on accepting and rejecting proposed moves in a domain. Where the probability criteria in the brute force method was just a uniform random number between 0 and 1, but now the physics behind the system applies to this criteria as well. The probability criteria s is now given by

$$s = \frac{G(x_p, x, \delta t)}{G(x, x_p, \delta t)} s_0 \quad (2.2.8)$$

Where s_0 is a random uniform number between 0 and 1 and $G(a, b, \delta t)$ is the so-called Green-function given by

$$G(a, b, \delta t) = \frac{1}{(4\pi D\delta t)^{3N/2}} \exp\left(-\frac{(a - b - D\delta t F(b))^2}{4D\delta t}\right) \quad (2.2.9)$$

Using this approach is what we will call the "Metropolis algorithm with importance sampling".

2.2.2.3 Application of the variational Monte Carlo method

As discussed in section 2.1.2 we need to solve the integral

$$\langle E_L \rangle = \int P(\vec{r}) E_L(\vec{r}) d\vec{r} \quad (2.2.10)$$

Where we have a trial function

$$\Psi_T(\vec{r}_0, \dots, \vec{r}_{N-1}, \alpha, \beta) \quad (2.2.11)$$

⁸Once again we refer to the lecture notes [2] for a more detailed explanation.

dependent on 2 trial parameters α and β where $\vec{r}_i = \begin{pmatrix} x_i \\ y_i \end{pmatrix}$. This is exactly the kind of problem the Metropolis algorithm can solve and the explicit algorithm for calculating $\langle E_L \rangle$ and $\langle E_L^2 \rangle$ is given in algorithm 2.1.

	Data:	An initial position matrix $\mathbf{r} = (\vec{r}_0, \vec{r}_1 \dots \vec{r}_{N-1}) = \begin{pmatrix} x_0 & x_1 & \dots & x_{N-1} \\ y_0 & y_1 & \dots & y_{N-1} \end{pmatrix}$	
		A method of choosing the step $\text{Method}(\mathbf{r}) = \Delta\vec{r} = \begin{pmatrix} \Delta x \\ \Delta y \end{pmatrix}$	
	Result:	The expectation value of the local energy: $\langle E_L \rangle$	
		The expectation value of the local energy squared: $\langle E_L^2 \rangle$	
1	begin		
2	<i>cumulative_local_energy</i> = $E_L(\mathbf{r}, \alpha, \beta)$	// Initialization	
3	<i>cumulative_local_energy_squared</i> = 0		
4	<i>counter</i> = 0		
5	while <i>counter</i> < M do		
6	<i>i</i> = randint(0, 1, ..., $N - 1$)	// Choose random element index	
7	$\Delta\vec{r} = \text{Method}(\mathbf{r})$	// Create a random two-dimensional step	
8	$\mathbf{r}_p = \begin{pmatrix} x_0 & x_1 & \dots & x_i + \Delta\vec{r} & \dots & x_{N-1} \\ y_0 & y_1 & \dots & y_i & \dots & y_{N-1} \end{pmatrix}$	// Create a trial position matrix	
9	<i>s</i> = prob_criteria(0,1)	// Generate a probability criteria	
10	<i>w</i> = $ \psi(\alpha, \beta, \mathbf{r}_p) ^2 / \psi(\alpha, \beta, \mathbf{r}) ^2$	// Calculate the probability ratio	
11	if <i>w</i> ≥ <i>s</i> then		
12	$\vec{r} = \vec{r}_p$		
13	$E_L(\mathbf{r}, \alpha, \beta) = \frac{1}{\Psi_T(\mathbf{r}, \alpha, \beta)} \hat{H} \psi_T(\mathbf{r}, \alpha, \beta)$	// Calculate the local energy	
14	end		
15	<i>cumulative_local_energy</i> $\pm E_L(\mathbf{r}, \alpha, \beta)$	// Update <i>cumulative_local_energy</i>	
16	<i>cumulative_local_energy_squared</i> $\pm E_L(\mathbf{r}, \alpha, \beta)^2$	// Update <i>cumulative_local_energy_squared</i>	
17	<i>counter</i> ± 1	// Update <i>counter</i>	
18	end		
19	Calculate $\langle E_L \rangle = \frac{\text{cumulative_local_energy}}{M}$		
20	Calculate $\langle E_L^2 \rangle = \frac{\text{cumulative_local_energy_squared}}{M}$		
21	end		

Algorithm 2.1: The metropolis algorithm used for finding the expectation value of the local energy and the expectation value of the local energy squared. "Method" refers to either the brute force approach or importance sampling.

If we move only one particle at a time, each new trial position will be given by

$$\mathbf{r}_p = \begin{pmatrix} x_0 & x_1 & \dots & x_i + \Delta\vec{r} & \dots & x_{N-1} \\ y_0 & y_1 & \dots & y_i & \dots & y_{N-1} \end{pmatrix} \quad (2.2.12)$$

Where $\mathbf{r} = \begin{pmatrix} x_0 & x_1 & \dots & x_{N-1} \\ y_0 & y_1 & \dots & y_{N-1} \end{pmatrix}$. If we are using the brute force approach, then $\Delta\vec{r}$ is simply

given by

$$\boxed{\Delta\vec{r} = \Delta r \cdot \vec{\text{rand}}} \quad (2.2.13)$$

Where Δr is a predefined step length and $\vec{\text{rand}}$ is a random 2-vector with elements between -1 and 1 .

If we want to implement importance sampling however, we need expressions for the terms in equation 2.2.7. These terms can be shown [1] to be

$$D = \frac{1}{2} \quad (2.2.14)$$

Which stems from the fact that the drift is caused by kinetic energy in front of which is a factor $\frac{1}{2}$ and

$$F = 2 \frac{1}{\Psi_T} \nabla_i \Psi_T \quad (2.2.15)$$

The formula for using importance sampling when choosing the trial position \mathbf{r}_p for our wave function is thus

$$\boxed{\Delta\vec{r} = \left(\frac{1}{\Psi_T} \nabla_i \Psi_T \right) \delta t + \eta} \quad (2.2.16)$$

We can rewrite this, as in section 2.1.3.4

$$\frac{1}{\Psi_T} \nabla_i \Psi_T = \frac{1}{|S_i|J} \nabla_i (|S_i|J) = \frac{1}{|S_i|J} (|S_i| \nabla_i J + J \nabla_i |S_i|) \quad (2.2.17)$$

$$\boxed{\frac{1}{\Psi_T} \nabla_i \Psi_T = \frac{\nabla_i |S_i|}{|S_i|} + \frac{\nabla_i J}{J}} \quad (2.2.18)$$

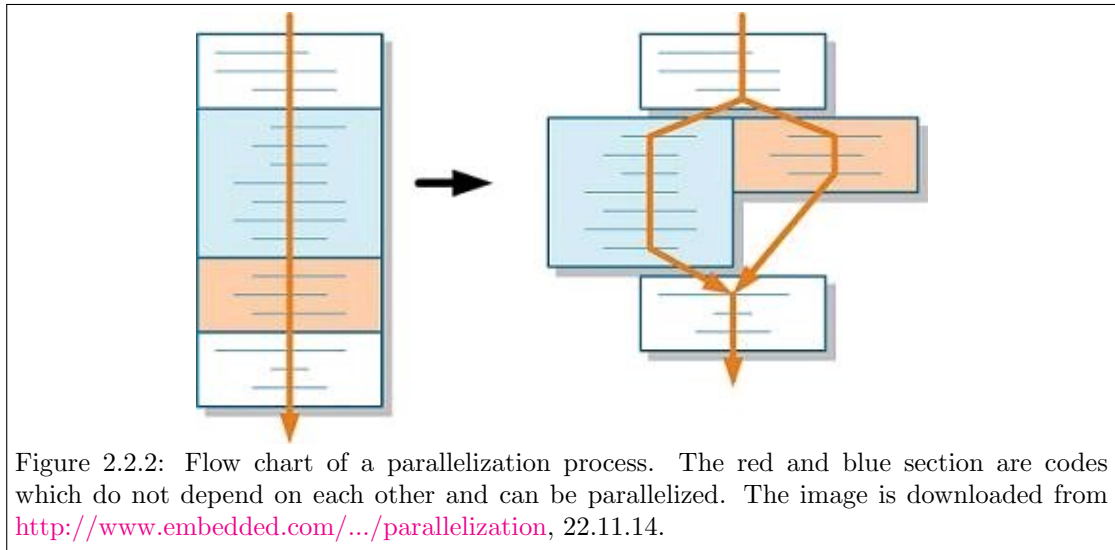
Expressions we can find both from numerical differentiation and from closed form expressions (equations 2.1.40). In this report, we will use both these approaches and compare the CPU time needed. Using the variational principle of quantum mechanics along with this Monte Carlo approach is what is known as the *variational Monte Carlo* method (or VMC for short). As we shall see, this is a powerful tool for investigating quantum mechanical systems.

2.2.3 Parallelization

Parallelization is a way of exploiting the multiple CPU's you find in modern computers. The idea behind is that tasks that are not dependent on each other and can be done in any order may be divided into so-called threads, and each thread can do its own task, see figure 2.2.2.

Using a library such as OpenMP⁹ (used in this project) makes use of all four CPU's if told to split the work into four different threads. Such an approach is easy to implement to this problem, because we can calculate $\langle E_L \rangle$ for different trial parameters at the same time.

⁹<http://openmp.org/wp/>



3 Experimental

3.1 Benchmarks and verification

3.1.1 Benchmarks for the brute force approach, no repulsion or Jastrow factor

As discussed in section 2.1.3.3, when $\omega = 1 \text{ Hz}_0$, the trial wave function should be able to reproduce the exact solution $E = 2 \text{ J}_0$ when we disregard the electron repulsion part of the Hamiltonian and don't include the Jastrow factor. This benchmark was tested¹⁰ with the brute force Metropolis method by varying α from 0 to 1.5 with steps of 0.05 using numerical differentiation of the wave function in the expression of the local energy. 10^7 Monte Carlo simulations were performed for each α with a step length Δr suited to each case to get an acceptance rate of around 0.5 (which is implemented in the code before the Monte Carlo simulation is started).

Then then the benchmarks for the $N = 6$ and $N = 12$ electron case was tested¹¹, still with the brute force approach and 10^7 Monte Carlo simulations for the $N = 6$ case and 10^6 for the $N = 12$ case, but this time with a smaller interval around $\alpha = 1$, ranging from 0.9 to 1.1 with steps of 0.05. In order to also verify the correct implementation of the oscillator frequency ω , this was set to 1.5 Hz_0 , so the energies to reproduce are $10\omega = 15 \text{ J}_0$ and $28\omega = 42 \text{ J}_0$.

3.1.2 Benchmark for the brute force approach, with repulsion and Jastrow factor

The exact energy of the two electron state *with* repulsion has been shown [4] to be 3ω . To test this result, first a fast investigation of $\langle E_L \rangle$ was performed as function of α and β to find the region in which the lowest energy is. Then, a more detailed search¹² was made with $\alpha \in [0.9, 1.1]$ and $\beta \in [0.35, 0.45]$, both in steps of 0.01 and 10^6 MC simulations at each step. The brute force approach with numerical evaluation of the local energy was used and ω was set to 1 Hz_0 . If the exact wave function were within our trial parameters, we would expect to get the exact answer $3 \cdot 1 = 3 \text{ J}_0$, but since this may not be the case we expect the lowest energy to be larger than this, according to section 2.1.2.2.

3.1.3 Comparison of different methods

As described in the theory section, a variety of different methods for solving the VMC problem has been explained. Firstly, there is a choice whether to use brute force (BF) or importance sampling (IS) when picking new trial positions in the metropolis algorithm. Secondly there is the possibility of using numerical methods (NLE) or the analytical expressions (ALE) when evaluating the local energy. In addition, if we're using importance sampling in the metropolis algorithm, there is a choice to whether or not we should use numerical (NQF) or analytical (AQF) expressions for the quantum force. All these methods should output the same result for the expectation value of the local energy, and to verify this an investigation¹³ of $\langle E_L \rangle$ with the different methods were performed for three different, semi-random¹⁴, combinations of problem

¹⁰/Logs/N2_norep_bruteforce_num/test_investigate.cpp, 21.11.14. See appendix, section B.

¹¹/Logs/N12_norep_bruteforce_num/test_investigate.cpp and /Logs/N6_norep_bruteforce_num/test_investigate.cpp, 21.11.14.

¹²/Logs/N2_rep_jast_num/test_investigate.cpp, 21.11.14.

¹³/Logs/compare_methods/first_example.cpp, second_example.cpp, third_example.cpp, 21.11.14.

¹⁴Chosen randomly by me, that is.

and trial function parameters; (Number of electrons N , α , Jastrow Factor on (Jn) or off (Jf), β , ω , Electron repulsion on (En) or off (Ef)) with 10^6 Monte Carlo simulations.

3.2 Optimization and differences

In this section the different optimization methods, such as the Jastrow factor, analytical expressions and importance sampling, was investigated. The investigation of these issues was based upon twelve test cases with two electrons for which the optimal parameters were found, the procedure is explained in the following section. Since the validity of the different methods were verified in section 3.1, the method which seemed most efficient was used. Therefore, if nothing else is written, the method used is the brute force method with analytical expressions for the local energy.

3.2.1 Test cases

The twelve test cases for this section were based on 6 different oscillator strengths ($\omega = 0.01, 0.1, 0.28, 0.5, 0.75, 1.0 \text{ Hz}_0$) and electron repulsion both with and without the Jastrow factor. For each test case, the optimal parameters of α and β was found by calculating the energies for α and β in range $[0, 1.2]$ with a resolution of 0.01 and 10^5 MC simulations. Then the parameters yielding the smallest energy was logged¹⁵.

3.2.2 Jastrow factor

When the repulsion part is present, we expect the Jastrow factor to improve the correlation (interaction) between the electrons, giving us a better (i.e. lower) estimate of the energy. We can measure the correlation by seeing how the lowest energy estimate changes with the Jastrow factor relative to without the Jastrow factor. This relative difference was calculated for each of the test cases.

3.2.3 Importance sampling

Using importance sampling introduces the dependence on δt when evaluating $\langle E_L \rangle$, as discussed in section 2.2.2.2. The dependence of the importance sampling method on δt was investigated¹⁶ for $10^3 - 10^6$ Monte Carlo simulations and $\delta t \in [10^{-6}, 10^2]$. Trial wave function parameters were chosen to be $\alpha = 0.72$ and $\beta = 0.24$ ¹⁷. For every time step δt , a brute force evaluation of the energy was also performed for comparison. The acceptance rate as a function of δt was also investigated¹⁸ with 10^7 Monte Carlo simulations.

¹⁵/Logs/find_parameters2/, 22.11.14.

¹⁶Logs/importance_sampling/, 24.11.14.

¹⁷Which is not close to an eigenstate of the system for which we found optimal parameters in section 4.1.2. This is important because if the parameters are such that we are close to an eigenstate, E_L will not vary much from point to point, which reduces the importance of good sampling.

¹⁸/Logs/IS_accept/IS_accept.cpp, 07.12.14.

3.2.4 Timely differences between methods

The time used by the different methods was investigated for $N = 2$ ¹⁹ and $N = 6$ ²⁰ electrons with some arbitrarily chosen values of α and β . The notation of the methods is described in section 3.1.3.

3.3 Applications

3.3.1 Properties of the approximated wave functions

Another six test cases and wave functions with 6 electrons were found²¹ using the same methods described in section 3.2.1²². Then five interesting properties of the 24 approximated wave functions found here and in section 4.2.1 was investigated²³ with 10^7 Monte Carlo simulations. These five interesting properties were

- The expectation value of the energy
- The variance of the local energy
- The expectation value of the average distance between electrons
- The expectation value of the potential energy of the system
- The expectation value of the kinetic energy of the system

3.3.2 The virial theorem

The virial theorem, as described in section 2.1.4, was tested for the optimal wavefunctions found in these earlier sections by plotting plotting the ratio of $\langle T \rangle$ to $\langle V \rangle$ as a function of ω . The different forms of energy were also found²⁴ for the no repulsion, no Jastrow factor case, for which the optimal parameter is $\alpha = 1$, as found in section 4.1.1, in order to test the virial theorem for these cases too.

¹⁹/Logs/times1/, 25.11.14.

²⁰/Logs/times2/, 25.11.14

²¹/Logs/find_parameters2/, 22.11.14.

²²For the $\omega = 0.01$ case, a manual search, as the one in section 3.1.2, had to be made when the result from the automated search yielded negative energies. /Logs/N6w001/, 28.11.14.

²³Logs/interesting_quantities, 29.11.14.

²⁴/Logs/interesting_quantities2, 29.11.14.

4 Results and discussion

4.1 Benchmarks and verification

4.1.1 Benchmarks for the brute force approach, no repulsion or Jastrow factor

Table 4.1.1 shows the results from the brute force simulation of the two electron - no repulsion case. A plot of the results is shown in figure 4.1.1.

α	0.0	0.05	0.1	0.15	0.2	0.25	0.3	0.35	0.40	0.45
$E[J_0]$	1.1e5	19.96	10.03	6.77	5.17	4.23	3.61	3.19	2.89	2.66
Variance[J_0^2]	7.4e9	2.0e2	4.8e1	2.0e1	1.1e1	7.0e0	4.5e0	3.1e0	2.2e0	1.5e0
α	0.5	0.55	0.6	0.65	0.7	0.75	0.8	0.85	0.9	0.95
$E[J_0]$	2.49	2.36	2.26	2.18	2.12	2.08	2.047	2.024	2.0096	2.002
Variance[J_0^2]	1.1e0	7.9e-1	5.6e-1	3.9e-1	2.6e-1	1.7e-1	1.0e-1	5.3e-2	2.6e-2	5.2e-3
α	1.0	1.05	1.1	1.15	1.2	1.25	1.3	1.35	1.4	1.45
$E[J_0]$	2	2.0029	2.010	2.021	2.035	2.05	2.07	2.09	2.12	2.14
Variance[J_0^2]	3.3e-13	4.7e-3	1.8e-2	3.9e-2	6.7e-2	1.0e-1	1.4e-1	1.8e-1	2.3e-1	2.9e-1

Table 4.1.1: Table showing the results from the brute force VMC simulation of the expectation value of the local energy $\langle E_L \rangle$ for α between 0 and 1.45 in the 2-electron case with no repulsion or Jastrow factor. The results show a minimum for the energy at $\alpha = 1$, as expected, and the variance at this point is so small that we expect it to be an eigenstate of the system. Units: see section 2.1.1.

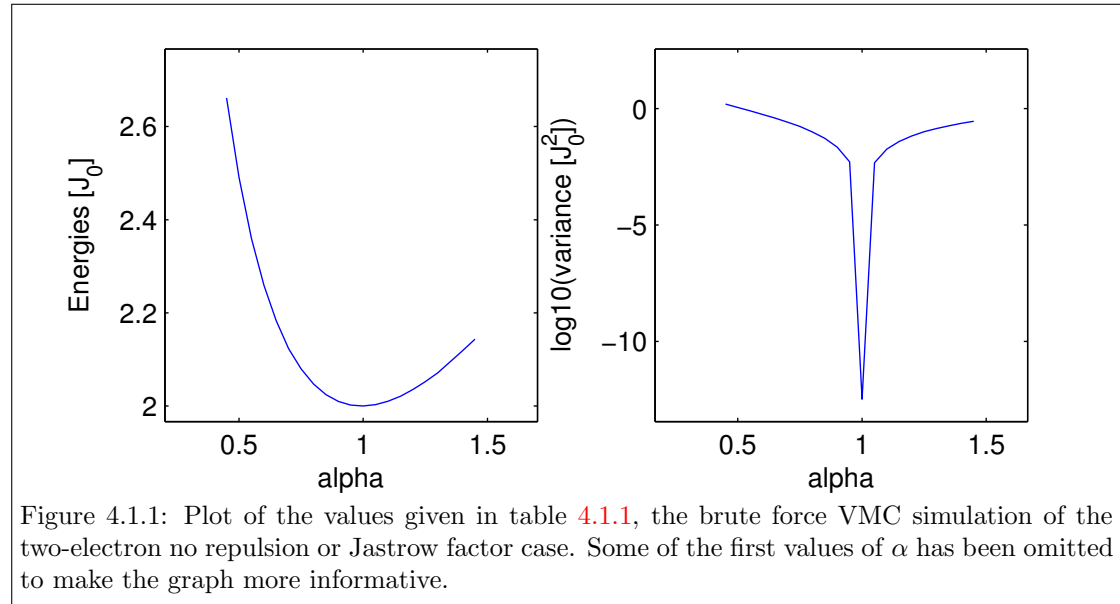


Figure 4.1.1: Plot of the values given in table 4.1.1, the brute force VMC simulation of the two-electron no repulsion or Jastrow factor case. Some of the first values of α has been omitted to make the graph more informative.

The figure shows exactly what we would expect from the discussion of section 2.1.3.3. The energy is always larger than $2 J_0$ and takes this value only when $\alpha = 1$. We also see a huge drop in the

variance just as we reach $\alpha = 1$ which indicates that this is indeed an eigenstate of the system. What little is rest of the variance at $\alpha = 1$ can be due to numerical errors in the calculation of the laplacians. This has in retrospect been verified to be true by using the analytical expression for the local energy.

Table 4.1.2 shows the result from the $N = 6$ and $N = 12$ electrons case with no repulsion using the brute force approach with numerical evaluation of the local energy.

N=6	α	0.9	0.95	1	0.105	0.11
	$E[J_0]$	15.0803	15.0850	15	15.0184	15.0708
	Variance[J_0^2]	2.49e-1	5.89e-2	2.56e-13	2.36e-2	2.05e-1
N=12	α	0.9	0.95	1	0.105	0.11
	$E[J_0]$	42.2114	42.0497	42	42.0563	42.1937
	Variance[J_0^2]	6.92e-1	1.66e-1	1.72e-10	1.48e-1	5.69e-1

Table 4.1.2: The results from calculating the expectation value of the local energy and its variance. We see that the code works for the $N = 6$ and $N = 12$ case because we are producing the expected results, $E_6 = 15 J_0$ and $E_{12} = 42 J_0$ ($\omega = 1.5 \text{ Hz}_0$). The variance at $\alpha = 1$ is so small that we probably have the exact wave function.

The table shows that we are able to produce the results we anticipated. Once again, we see a little variance at $\alpha = 1$ which is probably due the numerical evaluation of the local energy. The table also shows that the code has implemented the oscillator frequency ω correctly.

4.1.2 Benchmark for the brute force approach, with repulsion and Jastrow factor

A plot of the energies and \log_{10} of the variances after the investigation into finding the ground state energy for the $N = 2$ electrons, with repulsion and Jastrow factor, is shown in figure 4.1.2.

It is impossible to see from the figure what is the lowest energy, but manipulating the figure in matlab revealed the smallest test state energy, which is given in table 4.1.3.

The lowest energy $E = 3.00022 J_0$ and Variance = $0.001568 J_0^2$ at $\alpha = 0.98$ and $\beta = 0.42$.

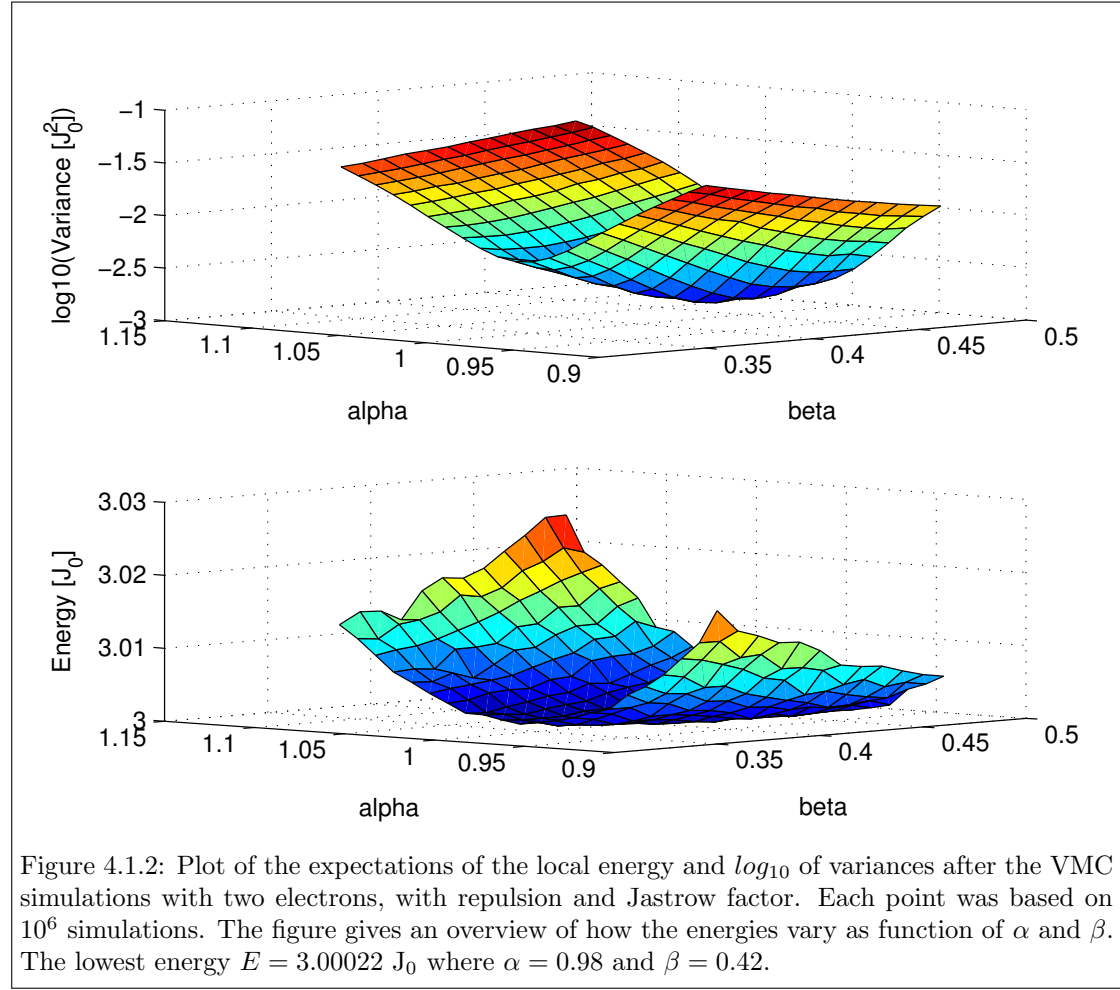
Table 4.1.3: The lowest energy found from the VMC study of the two electron case with repulsion and Jastrow factor.

The lowest energy was also found in the region where the variance was lowest. It seems thus that the value obtained in this VMC calculation is very close to the real lowest eigenstate. Very close, however, does not mean that we have found *the* eigenstate. As we saw in the previous section, when we hit the exact eigenstate, the variance dropped rapidly to sizes in order of magnitude $10^{-12} - 10^{-13}$ which was not the case here.

4.1.3 Comparison of different methods

The results from calculating $\langle E \rangle$ for the different method combinations and problem/wave function parameters are shown in table 4.1.4.

These are very strong results. Firstly, we have verified the numerical brute force method against known benchmarks and seen that they are correct, thus, it seems that the other methods are



Method parameters	Problem and wave function parameters		
	(2, 1, Jf, 0, 1, Ef)	(12, 0.5, Jf, 0, 1.5, En)	(6, 0.82, Jo, 0.22, 3, En)
(BF, NLE)	(2.000, 6e-13)	(92.10, 67.54)	(54.74, 28.11)
(BF, ALE)	(2.000, 0)	(92.18, 161.4)	(54.72, 28.19)
(IS, NLE, NQF)	(2.000, 6e-14)	(92.15, 66.43)	(54.72, 27.33)
(IS, NLE, AQF)	(2.000, 1e-13)	(92.06, 54.49)	(54.72, 27.32)
(IS, ALE, NQF)	(2.000, 0)	(92.13, 143.2)	(54.76, 27.35)
(IS, ALE, AQF)	(2.000, 0)	(92.12, 76.24)	(54.74, 27.44)

Table 4.1.4: A table of the expectation value and variance ($\text{Energy}[J_0]$, $\text{Variance}[J_0^2]$) of the local energy obtained with different problem/wave function parameters (N, α , J_n/J_f , β , ω , E_n/E_f). For explanation of abbreviations, see section 3.1.3. For all trials, 10^6 VMC calculations were performed and for the importance sampling methods, a time step of $\delta t = 0.1$ was used. The table shows that the different methods produce the same result.

working properly as well! Secondly, the different methods used very different ways to obtain the results. That the results are almost the same is a strong indication that all the methods are doing the same thing and functioning correctly.

4.2 Optimization and differences

4.2.1 Test cases

The results from finding the optimal parameters for α and β for the different test cases are given in table 4.2.1.

Test cases:	$\omega = 0.01 \text{ Hz}_0$		$\omega = 0.10 \text{ Hz}_0$		$\omega = 0.28 \text{ Hz}_0$	
Optimal parameters	No Jast.	Jast.	No Jast.	Jast.	No Jast.	Jast.
α	0.30	0.91	0.56	0.93	0.60	0.96
β	-	0.07	-	0.18	-	0.26
Energy[J_0]	1.03e-1	7.40e-2	5.25e-1	4.41e-1	1.14	1.02
Variance[J_0^2]	1.12e-2	1.48e-5	1.53e-1	2.76e-4	9.43e-1	7.05e-4

Test cases:	$\omega = 0.50 \text{ Hz}_0$		$\omega = 0.75 \text{ Hz}_0$		$\omega = 1 \text{ Hz}_0$	
Optimal parameters	No Jast.	Jast.	No Jast.	Jast.	No Jast.	Jast.
α	0.70	0.97	0.74	0.98	0.72	0.97
β	-	0.32	-	0.38	-	0.42
Energy[J_0]	1.80	1.66	2.50	2.34	3.15	3.00
Variance[J_0^2]	1.25	1.01e-3	1.69	1.35e-3	2.03	2.7e-3

Table 4.2.1: The optimal parameters with and without Jastrow factor (Jast.) for different oscillator potentials. Results were produced by calculating the energy for every α and β in the interval $[0, 1.2]$ with a step length of 0.01 and 10^5 MC simulation. The estimates with the Jastrow factor are better than those without.

The result for $\omega = 1 \text{ Hz}_0$ with Jastrow factor is almost in perfect agreement with what was found in section 4.1.2, even though the method of finding the optimal parameters was different. This indicates that the results obtained are reliable even though only 10^5 simulations were performed. For the purpose of this section, they are probably good enough.

Another approach to get these parameters would be to do a similar approach as in section 4.1.2 for each case. This proved to be too time-consuming, and an automated approach such as the one used here could be run overnight, which was done here. For a further discussion on code efficiency and time constraints, see section 4.2.5.

4.2.2 Jastrow factor

The relative change in energy (i.e. correlation) due to the Jastrow factor for the test cases is given in table 4.2.2.

A plot of the correlations in table 4.2.2 is given in figure 4.2.1.

Our first observation is that the Jastrow factor does indeed better our estimation of the ground state energy. We already knew from section 4.1.2 that the including the Jastrow factor gave us

ω	0.01	0.10	0.28	0.50	0.75	1
Correlation $C = \frac{E_{NJ} - E_I}{E_{NJ}}$	0.282	0.160	0.105	0.078	0.064	0.048

Table 4.2.2: The correlation introduced by the Jastrow factor for the optimal parameters α and β as a function of ω . We see that the correlation factor is less important for high oscillator potentials. "NJ" means no Jastrow factor and "J" means with Jastrow factor.

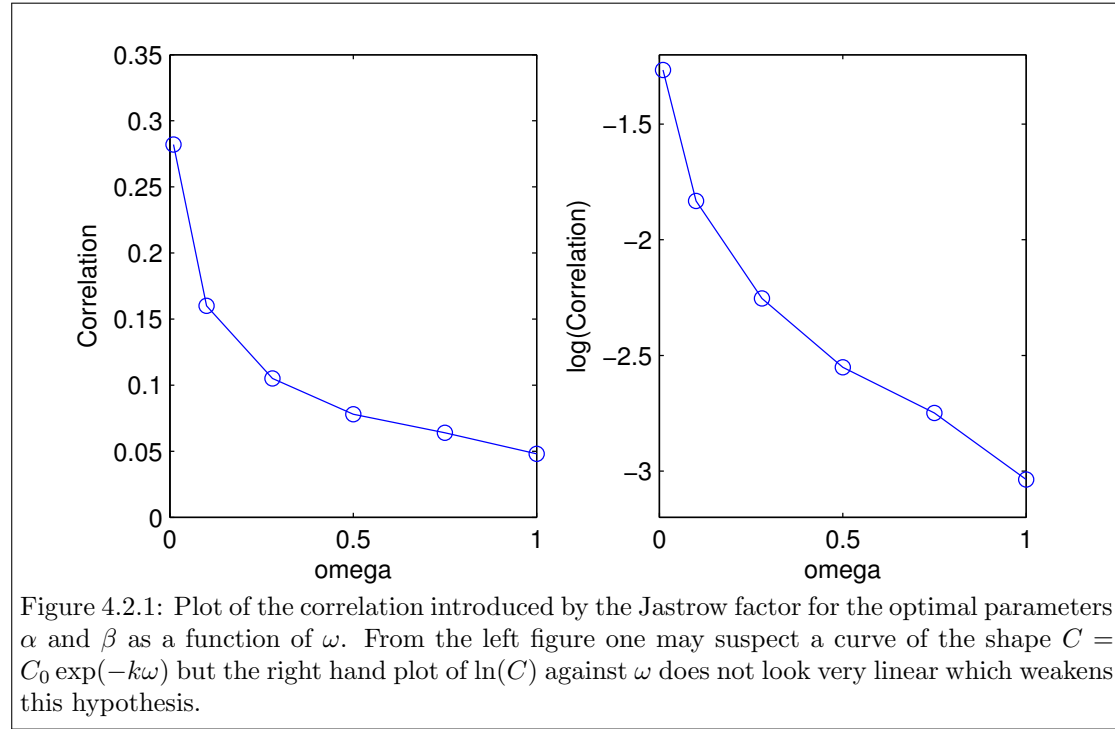


Figure 4.2.1: Plot of the correlation introduced by the Jastrow factor for the optimal parameters α and β as a function of ω . From the left figure one may suspect a curve of the shape $C = C_0 \exp(-k\omega)$ but the right hand plot of $\ln(C)$ against ω does not look very linear which weakens this hypothesis.

a very good estimate of the ground state energy when $\omega = 1$, and from table 4.2.1 we see that the ratio between variance and energy estimate is small and almost constant ($\sim 5 \times 10^{-4}$) in the case with the Jastrow factor as opposed to the case without the Jastrow factor.

Our second observation from both the table and the figure is that the correlations get smaller as the oscillator frequency increases. This is a counter-intuitive result. Normally one would expect the repulsion between the electrons to be more important the closer together the electrons are. One can try to explain the phenomenon by looking at another, equivalent expression of the expectation value of the local energy.

$$\langle E_L \rangle = \langle K \rangle + \langle V_{HO} \rangle + \langle V_{ER} \rangle \quad (4.2.1)$$

Where $\langle K \rangle$ is the expectation value of the kinetic energy, $\langle V_{HO} \rangle$ that of the harmonic oscillator potential and $\langle V_{ER} \rangle$ that of the electron repulsion potential. It seems that as ω increases, all these values increase, but the relative size of $\langle V_{ER} \rangle$ decreases, so for large ω , the role played by $\langle V_{ER} \rangle$ gets smaller and smaller.

From the left hand plot in the figure, one might suspect that the correlation decreases exponen-

tially as a function of ω . To test this, a plot of $\ln(C)$ against ω has been included in the right hand plot. If this hypothesis was true, the result should be a straight line, but alas, it is not. It is therefore probably some other rule governing the relation between C and ω .

4.2.3 Importance sampling

The results from evaluation of $\langle E_L \rangle$ as a function of Monte Carlo simulations and time steps δt are given in table 4.2.3 and figure 4.2.2.

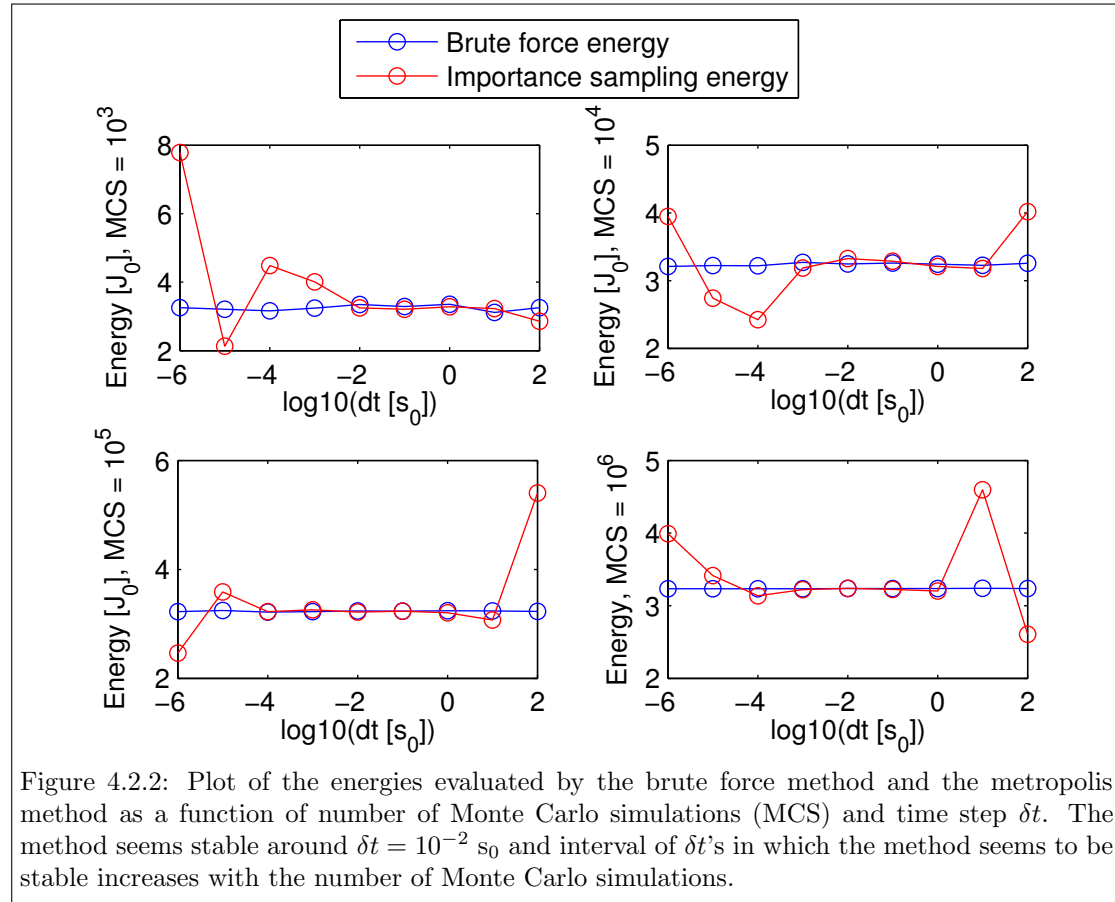
Energies obtained with the brute force method									
MCS $\backslash \delta t =$	10^{-6}	10^{-5}	10^{-4}	10^{-3}	10^{-2}	10^{-1}	1	10	10^2
10^3	3.26	3.21	3.16	3.24	3.35	3.29	3.36	3.11	3.25
10^4	3.21	3.22	3.22	3.27	3.25	3.26	3.24	3.22	3.26
10^5	3.23	3.24	3.21	3.22	3.24	3.23	3.24	3.24	3.23
10^6	3.23	3.23	3.23	3.23	3.24	3.24	3.24	3.24	3.24
Energies obtained with importance sampling									
MCS $\backslash \delta t =$	10^{-6}	10^{-5}	10^{-4}	10^{-3}	10^{-2}	10^{-1}	1	10	10^2
10^3	7.78	2.13	4.49	4.01	3.25	3.21	3.28	3.23	2.86
10^4	3.95	2.74	2.42	3.19	3.33	3.29	3.21	3.18	4.02
10^5	2.46	3.58	3.22	3.26	3.21	3.23	3.20	3.07	5.40
10^6	3.99	3.41	3.13	3.22	3.24	3.22	3.20	4.60	2.60

Table 4.2.3: Energies obtained with the brute force method and the importance sampling method as function of number of Monte Carlo simulations (MCS) and time step δt (in s_0). Brute force energy estimates do naturally not vary with δt since the latter do not play a role in the brute force method. The different energies obtained with the brute force method are thus only repetitions of the same simulation. Importance sampling seem to be stable around $\delta t = 10^{-2} s_0$.

We see from the results that the reliability of using importance sampling depends greatly on the time step chosen. The results seem to coincide with the brute force method when $\delta t \approx 10^{-2} - 10^{-1} s_0$. This is natural because if δt is too small, the steps in the metropolis algorithm does also become very small. It then takes a large number of Monte Carlo simulations for the metropolis walker to move across a representative selection of points. This is illustrated by the figure by noticing that as the number of Monte Carlo simulations gets larger, a greater range of δt 's converges to the proper solution. When δt gets too large, the step length gets too large and we have little control over how the energy estimates will behave.

The energy estimates by the brute force method does not vary with δt . This is natural because δt plays no role in the evaluation of $\langle E_L \rangle$ with the brute force method. The different energies obtained for different δt 's are thus just repetitions of the same measurement, and serve only as a illustration of the uncertainty in the evaluation of $\langle E_L \rangle$. For the purposes of this project, it seems that the brute force method serves as a stable and reliable method for calculating $\langle E_L \rangle$ with good precision only with 10^3 Monte Carlo simulations. For more complex problems, it may be that importance sampling, with its foundation in the physical system, attributes to greater precision in producing results, but for the problems discussed here, it seems that it only introduces a new uncertainty in whether the time step δt has been chosen correctly.

The acceptance rate of the importance sampling method as a function of the time step δt is given



in table 4.2.4.

$\delta t[s_0]$	10^{-6}	10^{-5}	10^{-4}	10^{-3}	10^{-2}	10^{-1}	1	10	10^2
AR:	1	1	1	0.99999	0.9997	0.991	0.769	0.00136	0

Table 4.2.4: The acceptance rate (AR) when using the metropolis algorithm as a function of δt . For a reasonably low time step, the acceptance rate is nearly at 100%, whereas it falls quickly down to zero once the timestep gets to big.

From the table, we see what we expected. For a small enough time step, the acceptance rate is nearly at 1 and as the time step gets too large, it falls to 0. Since we found the proper interval for δt to be between 10^{-2} and 10^{-1} , we can safely say that using the importance sampling method greatly increases the acceptance rate.

4.2.4 Timely differences between methods

Table 4.2.5 shows the time used by the different methods for the two different test cases. A plot of the times used are given in figure 4.2.3.

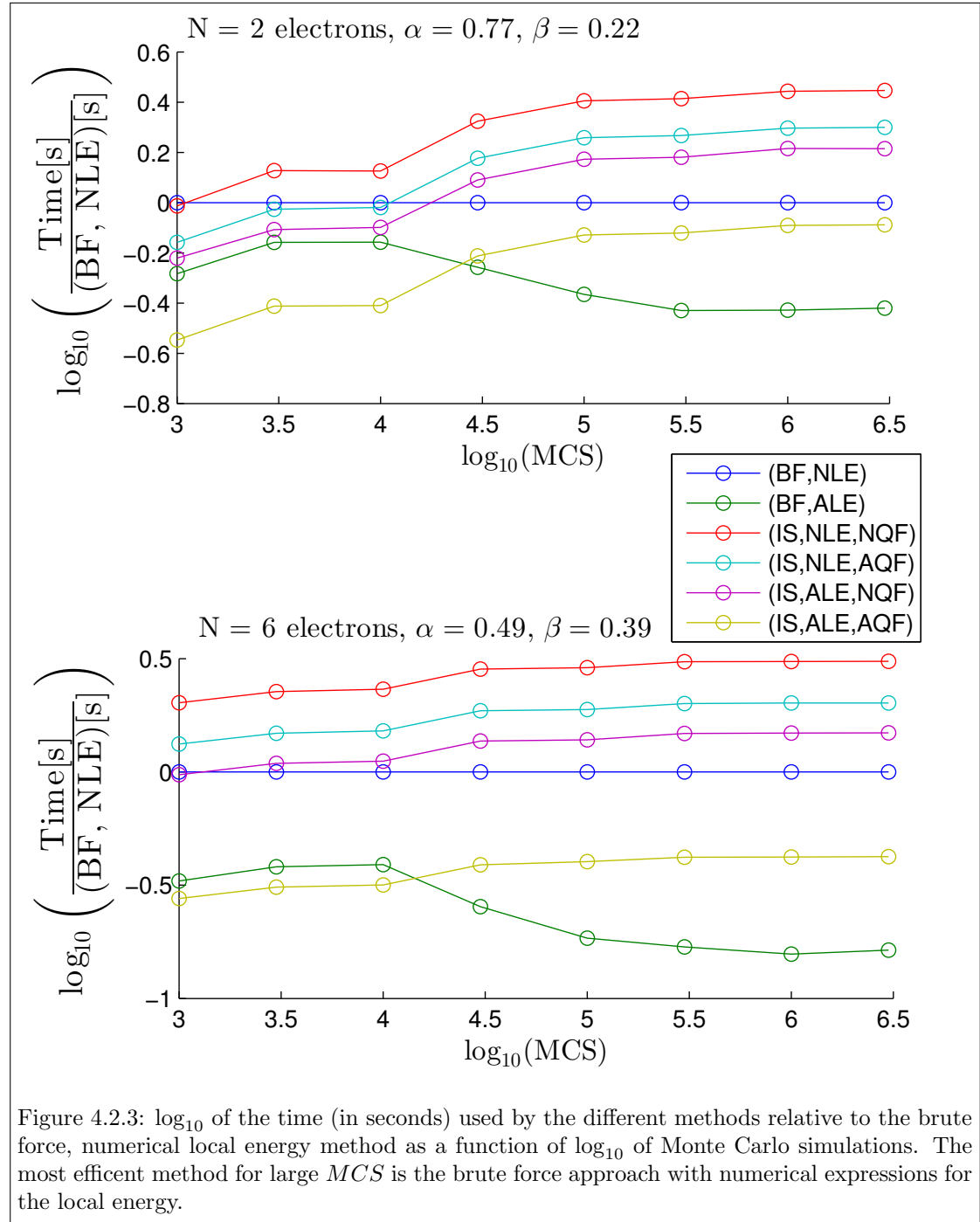
4.2 Optimization and differences

2 electrons with repulsion and Jastrow factor, $\alpha = 0.77$ and $\beta = 0.22$.								
Method \ MCS =	10^3	3×10^3	10^4	3×10^4	10^5	3×10^5	10^6	3×10^6
(BF, NLE)	1.87e-2	4.11e-2	1.36e-1	2.59e-1	7.14e-1	2.10	6.53	19.5
(BF, ALE)	9.75e-3	2.86e-2	9.45e-2	1.43e-1	3.08e-1	7.80e-1	2.44	7.39
(IS, NLE, NQF)	1.81e-2	5.52e-2	1.82e-1	5.46e-1	1.82	5.45	18.1	54.4
(IS, NLE, AQF)	1.30e-2	3.88e-2	1.30e-1	3.89e-1	1.29	3.88	12.9	38.8
(IS, ALE, NQF)	1.12e-2	3.22e-2	1.08e-1	3.19e-1	1.06	3.18	10.7	31.9
(IS, ALE, AQF)	5.30e-3	1.59e-2	5.28e-2	1.59e-1	5.30e-1	1.59	5.30	15.9
6 electrons with repulsion and Jastrow factor, $\alpha = 0.49$ and $\beta = 0.39$.								
Method \ MCS =	10^3	3×10^3	10^4	3×10^4	10^5	3×10^5	10^6	3×10^6
(BF, NLE)	1.44e-1	3.85e-1	1.25	3.06	10.0	28.4	94.3	283
(BF, ALE)	4.75e-2	1.47e-1	4.89e-1	7.79e-1	1.86	4.80	14.8	46.2
(IS, NLE, NQF)	2.91e-1	8.73e-1	2.91	8.71	29.1	87.1	290	870
(IS, NLE, AQF)	1.91e-1	5.71e-1	1.90	5.70	19.0	56.9	190	570
(IS, ALE, NQF)	1.40e-1	4.20e-1	1.40	4.19	14.0	42.0	140	420
(IS, ALE, AQF)	3.97e-2	1.20e-1	3.98e-1	1.19	4.05	11.9	39.7	120

Table 4.2.5: Time (in seconds) used by the different methods as a function of Monte Carlo simulations (MCS). See section 3.1.3 for method abbreviations. The CPU-time spent using analytical expression is dramatically reduced.

From the result we see that the relative difference in the time spent by the different methods stabilize after $\sim 10^5$ Monte Carlo simulations. After this point, the brute force metropolis algorithm with the analytical expression for the local energy is the most time efficient method, both for $N = 2$ and $N = 6$. For the $N = 6$ case, the latter method uses in fact almost as little as 1/20 of the time the slowest method (Importance sampling, numerical expressions) needs. To begin with, at 10^3 Monte Carlo simulations, importance sampling with analytical expressions is the fastest method. This is because the brute force method needs to run a couple of simulations without sampling to begin with in order to achieve the wanted acceptance rate of 0.5 whereas the importance sampling method can begin straight away sampling points. But as the number of Monte Carlo simulations increase however, this head start gets relatively smaller.

We also see that whenever analytical expressions is used instead of numerical ones, the efficiency is increased. From the figure we see that when using importance sampling, the implementation of the analytical local energy produces a greater increase in efficiency than implementing analytical expressions of the quantum force. And only when implementing both analytical expressions for the local energy *and* the quantum force is the importance sampling method superior to the brute force, numerical local energy method.



4.2.5 Discussion: code efficiency and time constraints

The code upon which this project is built has a lot of potential for improvement. Lots of the methods developed in this project has been programmed to the point at which the worked, and time constraints have cut short further improvements with regards to code efficacy. Examples of things that could have improved general code efficacy are things as

- **Reducing the amount of times a variable is calculated:** Although this aspect have been in the back of my mind while programming, I'm sure that a thorough review of the code would reveal a lot of potential.
- **Avoiding too many divisions:** Divisions in a computer is normally more slow than multiplication²⁵. Replacing recurrent divisions by clever multiplication might have improved code efficiency.
- **Reduce usage of complicated functions such as sin, exp etc:** Although I have put some thought into this while designing the code, there are probably some places where a lot of CPU time could be saved.

There are also things more specific to this project that could have improved code efficiency. Examples are

- **More efficient ratio calculations:** In the Metropolis algorithm used in this project, a ratio of the wave functions squared was evaluated. But since we only move *one* particle at a time, a lot of the so-called *co-factors* in the Slater determinant cancel²⁶ and reduces the number of expressions we need to calculate. If this were adjusted for, I think a lot of computational time could have been saved.
- **Re-usage of some expressions:** In the calculation of the analytical local energy, the terms needed for the analytical quantum force was also calculated. One could implement this into the code so that if the analytical expression for the local energy was evaluated *and* importance sampling was used with analytical quantum force, the expressions would reused and not calculated twice. There might also be other such examples of expressions which are evaluated multiple times in this code.
- **Better usage of OpenMP parallelization:** An interesting question is how much time it takes for OpenMP to communicate between the different threads. If this would prove itself a significant issue, then a better implementation of parallelization could have saved some time.

Finally there is the matter of method for finding the optimal parameters α and β . In this project, I used a very brute force method for which I could only spare 10^5 MC simulations for each energy in order for the process not to take weeks. A better algorithm for finding the optimal α and β was not in the scope of this project, but I believe it could seriously improve the efficacy of the process.

But all things considered, I am happy to have paid the price of a slow running code in exchange for having been able to implement lots of different methods for solving the problems discussed

²⁵Source: <http://streamcomputing.eu/>

²⁶Page 81, [3].

in this project. Even though the weak efficiency is probably affecting the precision of the result in the next section in a negative manner, the results are still correct within a certain margin of error. Also, the code is not going anywhere, so if I later want to improve upon it and implement better algorithms for finding α and β I am free to do so, even I don't have time to do so before the deadline of this project.

4.3 Applications

4.3.1 Properties of the approximated wave functions

The interesting properties of the approximated wave functions and the optimal variables for the six new test cases are given in table 4.3.1.

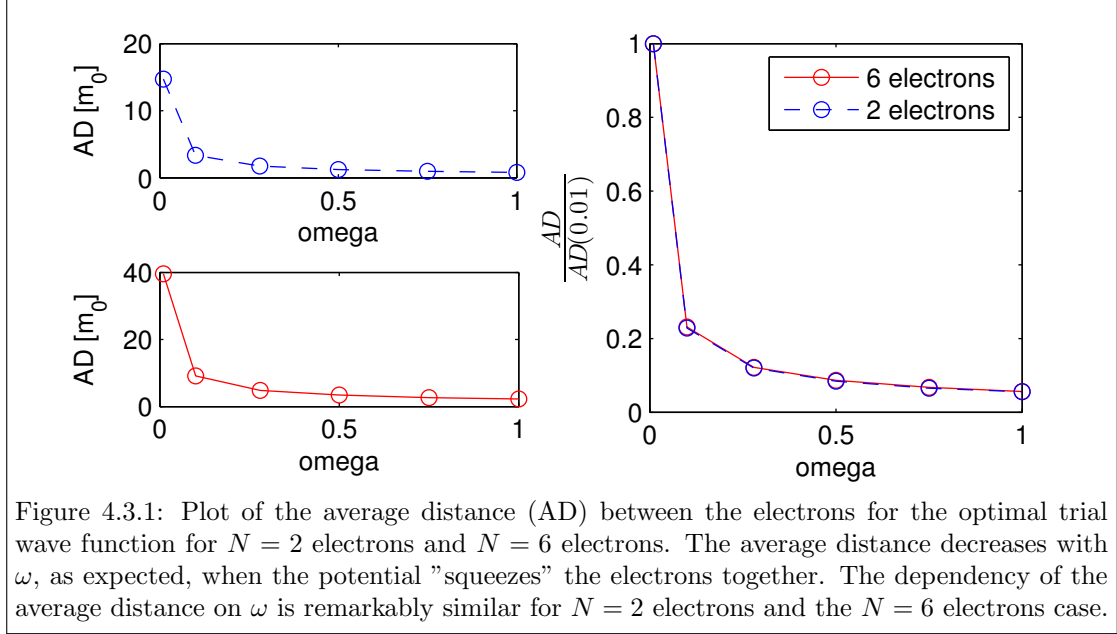
$N = 2$ electrons	$\omega = 0.01$	$\omega = 0.10$	$\omega = 0.28$	$\omega = 0.5$	$\omega = 0.75$	$\omega = 1$
Energy $\langle H \rangle$	7.40e-2	4.41e-1	1.02	1.66	2.34	3.00
Variance $[J_0^2]$	1.09e-5	2.74e-4	6.86e-4	1.03e-3	1.32e-3	1.78e-3
Average distance $[m_0]$	29.4	6.72	3.53	2.47	1.92	1.63
Potential Energy $\langle V \rangle$	6.43e-2	3.5e-1	7.71e-1	1.22	1.67	2.12
Kinetic Energy $\langle T \rangle$	9.74e-3	9.09e-2	2.51e-1	4.44e-1	6.70e-1	8.81e-1
$N = 6$ electrons	$\omega = 0.01$	$\omega = 0.10$	$\omega = 0.28$	$\omega = 0.5$	$\omega = 0.75$	$\omega = 1$
Optimal α	0.61	0.83	0.88	0.93	0.9	0.93
Optimal β	0.10	0.22	0.33	0.38	0.5	0.57
Energy $\langle H \rangle$	6.99e-1	3.57	7.62	11.8	16.1	20.2
Variance $[J_0^2]$	2.98e-4	4.52e-3	1.88e-2	4.59e-2	8.42e-2	1.33e-1
Average distance $[m_0]$	39.6	9.16	4.83	3.42	2.68	2.23
Potential Energy $\langle V \rangle$	6.71e-1	3.24	6.68	10.1	13.5	16.6
Kinetic Energy $\langle T \rangle$	2.76e-2	3.30e-1	9.56e-1	1.74	2.6	3.62

Table 4.3.1: The energies and average distances between the particles for the trial wave functions corresponding to the lowest expectation values of the local energy. The optimal wave function parameters used for the $N = 2$ electrons case are given in table 4.2.1. All energies are in units J_0 .

First of all, we notice that the energies obtained here, with 10^7 Monte Carlo simulations, is the same as the ones obtained in section 4.2.1 with 10^5 Monte Carlo simulations to the third digit. Which is an indication that 10^5 simulations to find α and β was not to little.

As we might expect, the higher the frequency of the oscillator potential, the closer the electrons are to each other. This is because the electrons are "squeezed" together by the potential. A plot of the average electron distance for both $N = 2$ electrons and $N = 6$ electrons as a function of ω is given in figure 4.3.1.

From the figure we see that the shape of the average distance's dependence on ω is remarkably similar for the two cases. A possible explanation of this fact is to consider the electrons as localized charges pushing each other away until the point where the curvature of the potential equals the repulsive pushing. The electrons would in this image form some sort equilateral shape which would not be dependent on the frequency of the oscillator and an increase in the oscillator would just reduce the "scale" of the pattern by a factor. That this "factor" is the same for the



$N = 2$ and the $N = 6$ electron case is not obvious, but not unreasonable²⁷ either. The fact that such a model can be applied to quantum mechanics however, is more surprising.

4.3.2 The virial theorem

A more detailed overview of the different expectation values of energies for the wavefunctions investigated in the previous section is given in table 4.3.2.

A plot of the ratio between the expectation value of the kinetic and the potential energy is given in figure 4.3.2.

From the figure and table, we see that the virial theorem holds very well for the no repulsion case. This is not surprising since as we know, we had the exact ground state. There does however seem to be a small favorization of kinetic energy over potential energy which is most important for the $N = 2$ electron case. The reason for this, I believe, has to do with the sampling technique. The wave function is constructed in such a way that kinetic energy is most important when the distance from the origin is small and potential energy is more important for larger distances. This means that we may have a small over representation of the "small distance to the origin"-points in our Monte Carlo simulation. The reason for this might be due to the fact that our starting point *is* one close to the origin. Another possible reason is that since we have a finite number of Monte Carlo points, some of the points *very* far away from the origin will not be reached in a finite simulation, resulting in no representation of these points whereas they should have been represented to a small degree in a perfect integration. These explanations do not, however, explain why for the $N = 6$ electron, no repulsion case, the same number of simulations seem to give better results. This might be due to the fact that the energy is greater with 6 electrons, reducing the relative impact of the small misrepresentation in the sampling points.

The other important thing to see is that the virial theorem is not fulfilled for the no repulsion

²⁷I'm sure one could make some geometric argument as to why this is the case.

4.3 Applications

$N = 2$ electrons, with repulsion and Jastrow factor.						
	$\omega = 0.01$	$\omega = 0.10$	$\omega = 0.28$	$\omega = 0.5$	$\omega = 0.75$	$\omega = 1$
Harmonic Energy $\langle V_{HO} \rangle$	2.82e-2	1.80e-1	4.24e-1	7.01e-1	9.91e-1	1.30
Repulsive Energy $\langle V_{RE} \rangle$	3.61e-2	1.71e-1	3.48e-1	5.15e-1	6.82e-1	8.16e-1
Potential Energy $\langle V \rangle$	6.43e-2	3.5e-1	7.71e-1	1.22	1.67	2.12
Kinetic Energy $\langle T \rangle$	9.74e-3	9.09e-2	2.51e-1	4.44e-1	6.70e-1	8.81e-1
$N = 6$ electrons, with repulsion and Jastrow factor.						
	$\omega = 0.01$	$\omega = 0.10$	$\omega = 0.28$	$\omega = 0.5$	$\omega = 0.75$	$\omega = 1$
Harmonic Energy $\langle V_{HO} \rangle$	2.30e-1	1.26	2.81	4.52	6.31	7.80
Repulsive Energy $\langle V_{RE} \rangle$	4.41e-1	1.98	3.87	5.55	7.22	8.77
Potential Energy $\langle V \rangle$	6.71e-1	3.24	6.68	10.1	13.5	16.6
Kinetic Energy $\langle T \rangle$	2.76e-2	3.30e-1	9.56e-1	1.74	2.68	3.62
$N = 2$ electrons, without repulsion or Jastrow factor.						
	$\omega = 0.01$	$\omega = 0.10$	$\omega = 0.28$	$\omega = 0.5$	$\omega = 0.75$	$\omega = 1$
Potential Energy $\langle V \rangle$	9.94e-3	9.95e-2	2.78e-1	4.97e-1	7.46e-1	9.95e-1
Kinetic Energy $\langle T \rangle$	1.01e-2	1.01e-1	2.82e-2	5.03e-1	7.54e-1	1.01
$N = 6$ electrons, without repulsion or Jastrow factor.						
	$\omega = 0.01$	$\omega = 0.10$	$\omega = 0.28$	$\omega = 0.5$	$\omega = 0.75$	$\omega = 1$
Potential Energy $\langle V \rangle$	5.00e-2	4.99e-1	1.40	2.50	3.74	4.99
Kinetic Energy $\langle T \rangle$	5.00e-2	5.00e-1	1.40	2.50	3.76	5.00

Table 4.3.2: The different forms of energies (in J_0) in the optimal wave functions for $N = 2$ and $N = 6$, with and without the Jastrow factor, as a function of ω .

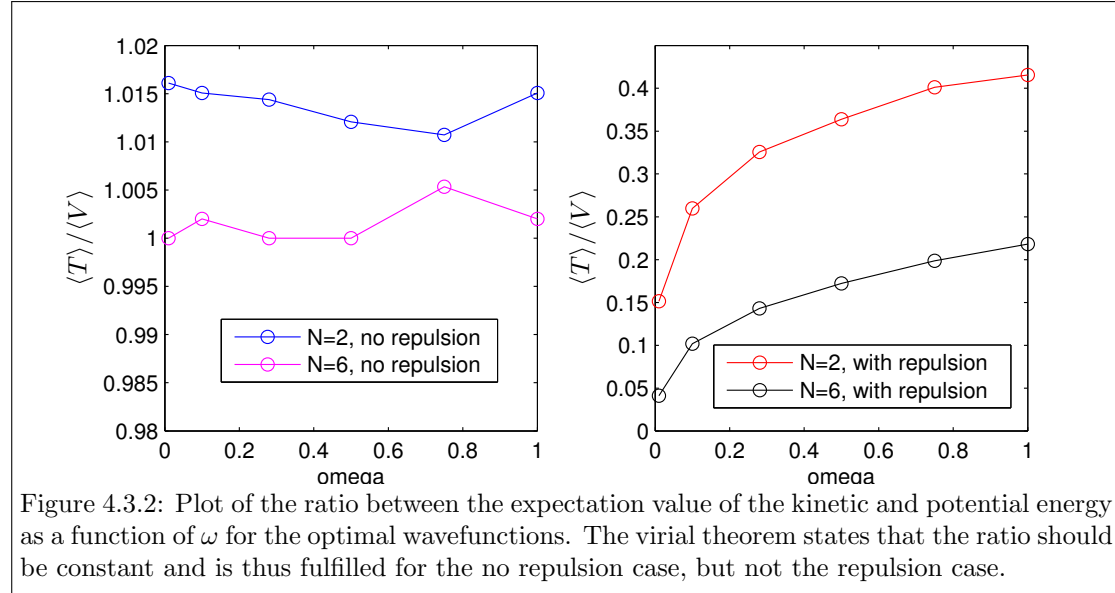


Figure 4.3.2: Plot of the ratio between the expectation value of the kinetic and potential energy as a function of ω for the optimal wavefunctions. The virial theorem states that the ratio should be constant and is thus fulfilled for the no repulsion case, but not the repulsion case.

cases. Here, the ratio between $\langle T \rangle$ and $\langle V \rangle$ is dependent on ω in such a way that when ω gets smaller, the potential term is much larger than the kinetic term. This is a very interesting observation. The kinetic energy is a measure of how much movement there is in the substance (here: electrons in a trap). Thus, if the kinetic energy is small compared to the potential energy, this means that the electrons are very immobile and localized, in the same way that freezing water causes molecules to stay put in one place. Does this mean that a small oscillator potential "freezes" the electrons in place, or is this solely an artifact of the numerical method? If it really is another "phase", what then are the properties of this substance? These are all fascinating questions which would be interesting to investigate another time.

5 Conclusion

We have seen in this project how the Monte Carlo method is an efficient tool to find a correct upper bound of ground state energies. The report shows how the implementation of different variations of the method has produced the same results, but in very different time scales as the most efficient method proved to be almost 20 times faster than the least efficient one.

One of the most striking discoveries was how the mean distance between the electrons seemed to follow a very specific pattern, not dependent on how many electrons there were in the trap to begin with. Further investigation of this property would be a fine project for another time.

Another striking discovery is how the importance of the electron-electron repulsion correlation varies as a function of the oscillator strength ω . Whereas one might expect the importance to get bigger as the electrons were "squeezed" together (i.e. strong oscillator potential), it turned out that this was not the case at all. At large values of ω , the repulsion correlation got less important and the dominant factor was the potential of the oscillator itself. For smaller values of ω however, it seemed that the electron correlations got more important and the investigation of the virial theorem revealed that the kinetic energy "drowned" in comparison to the potential energy. Since kinetic energy is a measure of how much the electrons are moving, this means that they became more stationary, localized, at small ω 's. One might say that the electrons "froze in place". This could be the introduction of more solid phase for the electrons, with perhaps many interesting qualities that could also make for a great continuation project.

I am often baffled by the efficiency of computational methods when applied to problems where analytical math does not get us anywhere. Finding the analytical solution to the 2-electron quantum dots problem was a great achievement credited to M. Taut [4], but in this project, less than 2000 lines of code was needed to get almost the exact same value for the energy, which in my opinion, is quite astounding.

References

- [1] Morten Hjorth-Jensen. Additional slides for monte carlo project. <http://www.uio.no/.../montecarloaddition.pdf>, 2014.
- [2] Morten Hjorth-Jensen. *Computational Physics - Lecture Notes Fall 2014*. August 2014.
- [3] Jørgen Høgberget. Quantum monte-carlo studies of generalized many-body systems, June 2013.
- [4] M. Taut. Two electrons in an external oscillator potential: Particular analytic solutions of a coulomb correlation problem. *Phys. Rev. A*, 48:3561–3566, Nov 1993.

A Reference to the questions posed in the project instructions

Since the format of this report does not correspond to the structure of the project instructions, a reference list over the posed questions and where to find the answer is given below.

	Instruction	Section[s]
a)	If we only include ... the energy is 2 a.u. Convince yourself that ... is simply 2ω . What is the total spin ...? Find arguments for why...	4.1.1 2.1.3.3 2.1.3.3
b)	Perform a Variational Monte Carlo calculation... You should parallize your program. Find the energy minimum. Compute also the mean distance...	4.1.2 2.2.3 , B 4.1.2 4.3.1
c)	Introduce now importance ... eventual differences.	4.2.3 , 4.1.3 , 4.2.4
d)	Compute the expectation ... and $\omega = 1.0$. How important are ... the Jastrow factor?	4.3.1 4.2.2
e)	Compute... for $N = 6$ electrons ... and $\omega = 1.0$. Reproduce the unperturbed ... is switched off. Convince yourself ... for $N = 6$ is 10ω . What is the expected total spin of the ground states?	4.3.1 4.1.1 2.1.3.3 2.1.3.3
f)	Use your optimal results ... comment your results.	4.3.2
g)	Find closed-form expressions... compare the results ... for both $N = 2$ and $N = 6$	2.1.3.4 4.2.4

Table A.0.3: Reference list over the posed questions and where to find the answer.

B Code

All codes used in this exercise can be found at GitHub:

<https://github.com/vidarsko/Project3>.

The main files are the header file "project3lib.h" and source file "project3lib.cpp". The class structure of the code is given in the bullet points below

- **TrialWavefunction:** A class for storing parameters (α , β , number of particles etc.) of the trial wave function and all the functions (Hermite polynomials, $n_x(i)$ etc.) in order to call the function properly.
- **QuantumDots:** A class in which the parameters (ω , number of particles, repulsion on/off etc.) of the system was stored. The different Monte Carlo methods were also part of this class and all the functions (local energy function, quantum force function etc.) needed to execute them properly.
- **Investigate:** A class with different investigation functions (for such things as finding the optimal parameters, comparing times etc.) made in order to easily run simulations for different input parameters. Most of the solve functions made use of parallelization. For example in order to find the expectation value of the energy for different trial wave function parameters at the same time. The parallelization was implemented using OpenMP in the simplest way through a parallelized "for"-loop. Using four threads, 100% of the CPU of my computer was used as opposed to 25% when not using parallelization, suggesting that it worked properly.

Throughout this report, reference to different codes are made as footnotes together with the date at which they were run.